https://doi.org/10.1093/plphys/kiac406 PLANT PHYSIOLOGY 2022: 190: 2651–2670

Plant Physiology®

Research Article

GA signaling expands: The plant UBX domain-containing protein 1 is a binding partner for the GA receptor

Amber L. Hauvermale [1,2], Jessica J. Cárdenas [3,4], Sebastian Y. Bednarek [3,4,*] and Camille M. Steber [1,2,5,*]

1 Department of Crop and Soil Sciences, Washington State University, Pullman, Washington, USA
2 Molecular Plant Sciences, Washington State University, Pullman, Washington, USA
3 Department of Biochemistry, University of Wisconsin-Madison, Madison, Wisconsin 53706, USA
4 Integrated Program in Biochemistry, University of Wisconsin-Madison, Madison, Wisconsin 53706, USA
5 Wheat Health, Genetics and Quality Unit, USDA-ARS, Pullman, Washington, USA

*Author for correspondence: sybednar@wisc.edu (S.Y.B.), camille.steber@usda.gov (C.M.S.)
These authors contributed equally (A.L.H. and J.J.C.).
A.L.H., J.J.C., S.Y.B., and C.M.S. conceived the study and designed the experiments. A.L.H and J.J.C. carried out the experiments. A.L.H., J.J.C., S.Y.B., and C.M.S. analyzed the data. A.L.H., J.J.C., S.Y.B., and C.M.S. wrote the article.
The authors responsible for distribution of materials integral to the findings presented in this article in accordance with the policy described in the Instructions for Authors (https://academic.oup.com/plphys/pages/general-instructions) are Camille Steber (camille.steber@usda.gov) and Sebastian Bednarek (sybednar@wisc.edu).

Abstract

The plant Ubiquitin Regulatory X (UBX) domain-containing protein 1 (PUX1) functions as a negative regulator of gibberellin (GA) signaling. GAs are plant hormones that stimulate seed germination, the transition to flowering, and cell elongation and division. Loss of Arabidopsis (*Arabidopsis thaliana*) *PUX1* resulted in a "GA-overdose" phenotype including early flowering, increased stem and root elongation, and partial resistance to the GA-biosynthesis inhibitor paclobutrazol during seed germination and root elongation. Furthermore, GA application failed to stimulate further stem elongation or flowering onset suggesting that elongation and flowering response to GA had reached its maximum. GA hormone partially repressed PUX1 protein accumulation, and PUX1 showed a GA-independent interaction with the GA receptor GA-INSENSITIVE DWARF-1 (GID1). This suggests that PUX1 is GA regulated and/or regulates elements of the GA signaling pathway. Consistent with *PUX1* function as a negative regulator of GA signaling, the *pux1* mutant caused increased GID1 expression and decreased accumulation of the DELLA REPRESSOR OF GA1-3, RGA. PUX1 is a negative regulator of the hexameric AAA+ ATPase CDC48, a protein that functions in diverse cellular processes including unfolding proteins in preparation for proteasomal degradation, cell division, and expansion. PUX1 binding to GID1 required the UBX domain, a binding motif necessary for CDC48 interaction. Moreover, PUX1 overexpression in cell culture not only stimulated the disassembly of CDC48 hexamer but also resulted in co-fractionation of GID1, PUX1, and CDC48 subunits in velocity sedimentation assays. Based on our results, we propose that PUX1 and CDC48 are additional factors that need to be incorporated into our understanding of GA signaling.

Received June 06, 2022. Accepted July 19, 2022. Advance access publication September 23, 2022
Published by Oxford University Press on behalf of American Society of Plant Biologists 2022.

Introduction

The gibberellins (also called gibberellin A or GAs) are a family of tetracyclic diterpenoid molecules, a subset of which function as phytohormones to stimulate seed germination, the transition to flowering, and growth via increased cell division and elongation (reviewed in Hauvermale et al., 2012). The role of GA in regulating physiological responses has been established by investigating phenotypes that occur in the absence of GA biosynthesis. For example, the GA biosynthesis deficient mutants, Arabidopsis (*Arabidopsis thaliana*) *ga1-3* and the tomato (*Solanum lycopersium*) *gib-1*, exhibit failure to germinate, dwarfed stature, defects in the transition to flowering, and infertility (Koornneef and Vanderveen, 1980; Karssen et al., 1989). All phenotypes that are present in GA biosynthetic mutants are rescued with GA application, demonstrating the role that GA hormone signaling plays in the regulation of developmental events, which ensure plant species survival.

Seed dormancy is an evolutionary adaptation that ensures species survival by regulating germination timing to coincide with optimal growing conditions. Two hormone signaling pathways regulate a seed's transition from dormancy, the inability to germinate, to a state of increased germination potential. Abscisic acid (ABA) establishes seed dormancy during embryo maturation and maintains dormancy in mature seeds. GA signaling breaks seed dormancy and stimulates germination (Koornneef et al., 1982; reviewed by Finkelstein et al., 2008). Dormancy-breaking treatments like after-ripening (dry storage) and cold stratification (cold imbibition) weaken dormancy by modulating endogenous levels of and sensitivity to ABA and GA hormones (Derkx et al., 1994; Seo et al., 2009; Yamauchi et al., 2004). After-ripening and cold stratification also work additively to break seed dormancy and to synchronize germination (Foley and Fennimore, 1998).

Previous work has indicated that GA stimulates GA responses via destruction of DELLA (Asp–Glu–Leu–Leu–Ala) domain proteins, negative regulators of GA responses, through the ubiquitin–proteasome pathway (reviewed by Nelson and Steber, 2016; Thomas et al., 2016). GA binding to the GA-INSENSITIVE DWARF1 (GID1) GA receptors results in a conformational change that creates a DELLA-binding domain. Subsequently, formation of the GID1–GA–DELLA complex allows for recognition of DELLA proteins by the Arabidopsis SLEEPY1 (SLY1) F-box protein. The Skp1-Cullin-F-box (SCF^{SLY1}) E3 ubiquitin-ligase catalyzes DELLA polyubiquitylation, thereby targeting DELLA for destruction by the 26S proteasome (Griffiths et al., 2006; Murase et al., 2008; Shimada et al., 2008; Ueguchi-Tanaka and Matsuoka, 2010).

There are three homologous GA receptors in Arabidopsis, GID1a, b, and c that function to bind GA and transduce the GA signal; however, GID1b has unique properties (Nakajima et al., 2006; Yamamoto et al., 2010). The protein sequences for GID1a and GID1c are more closely related to each other than to GID1b. GID1a has 85% amino acid identity with GID1c, but only 66% identity with GID1b (reviewed by Nelson and Steber, 2016). GID1b has higher affinity than GID1a and GID1c for GA and DELLA, and has the unique ability to bind DELLA in the absence of GA (Nakajima et al., 2006; Yamamoto et al., 2010). Even in the absence of GA (i.e. *ga1-3* or in the shoot apical meristem), GID1b is able to bind to DELLA and likely provides a basal level of GA-independent signaling. However, GA enhances GID1b affinity for DELLA, indicating that the receptor is GA responsive (Yamamoto et al., 2010). Interestingly, phenotypic characterization revealed that *GID1b* can behave both as a positive and negative regulator of germination and stem elongation, whereas *GID1a* and *GID1c* behave as positive regulators of germination (Ge and Steber, 2018).

The *sly1* F-box mutant is unable to destroy DELLA protein and shows GA-insensitive phenotypes including failure to germinate, dwarfism, delayed flowering, and reduced fertility (Steber et al., 1998; McGinnis et al., 2003). These *sly1* phenotypes, however, can be partially rescued by GA application and overexpression of the *GID1* GA receptors (Ariizumi and Steber 2007, Ariizumi et al., 2008, 2013). This GA- and *GID1*-dependent rescue of the *sly1* phenotypes does not result in DELLA protein destruction. A similar rescue of the F-box mutant *gid2* was observed in rice (Ueguchi-Tanaka et al., 2008). Collectively, these results suggested that some aspects of GA signaling occur independently of DELLA destruction, possibly through GID1 interaction with other regulatory proteins (Ariizumi et al., 2013; Hauvermale et al., 2015). In this study, we identified plant Ubiquitin Regulatory X (UBX) domain-containing protein 1 (PUX1), a Cell Division Cycle 48 (CDC48) regulating protein in Arabidopsis, as a GID1-interacting protein. This study takes the first steps toward investigating whether PUX1 provides an alternative pathway for GA signaling. Our findings indicate that PUX1 negatively regulates GA responses including seed germination, root growth, and flowering.

CDC48 (also known as p97/Vasolin-containing protein, VCP) is a highly conserved homohexameric AAA + ATPase that unfolds/extracts proteins associated with soluble or membrane-associated protein complexes involved in a variety of essential cellular functions required for cellular homeostasis including: (1) cell cycle regulation; (2) endoplasmic reticulum-associated degradation; (3) membrane biogenesis; (4) protein turnover via the ubiquitin–proteasome pathway; (5) autophagosome biogenesis; and 6) maintenance of DNA integrity (reviewed in Hoppe et al., 2000; Meyer et al., 2002; Woodman, 2003). In Arabidopsis, there are three genes encoding CDC48 homologs, *AtCDC48a*, *AtCDC48b*, and *AtCDC48c* (Rancour et al., 2002). Disruption of *AtCDC48a* results in pleiotropic developmental defects in embryogenesis, seedling growth, and pollen tube growth likely through its activity in cell division and elongation (Park et al., 2008).

The Arabidopsis PUX1 protein regulates CDC48 function in plant growth and cell elongation (Rancour et al. 2004). In order for CDC48/p97 to fulfill its many functions it

associates with different cofactors, including members of the UBX domain family, that recruit the ATPase to specific cellular processes (Meyer et al., 2002; Schuberth and Buchberger, 2008; Zhang et al., 2021). However, unlike other UBX-domain proteins that facilitate the interaction of CDC48 with client proteins (Gallois et al., 2013; Kretzschmar et al., 2018; Marshall and Vierstra, 2019), PUX1 binding to CDC48 promotes the disassembly of active hexameric complexes to ATPase-inactive subunits (Rancour et al., 2004; Park et al., 2007). Loss of *PUX1* results in enhanced growth phenotypes in Arabidopsis (Rancour et al., 2004) that are similar to GA-induced root and shoot growth.

This study identified PUX1 as a GID1-interacting protein, suggesting that PUX1 plays a role in GA hormone signaling. Consistent with this, *pux1* mutants displayed "GA overdose" phenotypes similar to mutations in the negative regulator of GA signaling, Arabidopsis *SPINDLY* (Jacobsen and Olszewski, 1993). The *pux1* mutants exhibited decreased sensitivity to the GA biosynthesis inhibitor paclobutrazol (PAC) during seed germination and root elongation. Moreover, *pux1* mutants showed increased stem elongation and early flowering. GID1 protein interacts with PUX1 in a GA-independent manner both in vivo and in vitro. Interestingly, GA appears to regulate the levels of PUX1 protein, whereas mutations in *PUX1* altered expression of GA signaling genes. Collectively, these results suggest that the GID1–PUX1 protein interaction plays a functional role in GA signaling.

Results

Identification of PUX1 as a GID1-interacting protein

Given that GID1 receptor signaling can be independent of DELLA destruction (Ariizumi et al., 2008, 2013), we hypothesized that GID1 likely interacts with other growth-regulating proteins. To examine this, a yeast two-hybrid screen for seed-expressed GID1 interactors was conducted. GID1b was chosen for use as bait because *GID1b* overexpression more strongly rescued the poor germination and dwarfism phenotypes of *sly1* (Ariizumi et al., 2008, 2013). Yeast was transformed with an in-frame fusion of GID1b to the Gal4 DNA-binding domain (GID1b–Gal4db) as bait and a seed-specific Arabidopsis cDNA library fused to the activation domain of the yeast Gal4 transcription factor (Gal4ad) (Supplemental Table S1; see "Materials and methods"). A total of 132 clones showed interaction with *GID1b* upon retest in the yeast two-hybrid system (Supplemental Table S2). Among the best *GID1b*-interacting candidates were a GA-responsive gene, *GASA6* (At1G74670; *GA-Stimulated Arabidopsis Protein 6*) (Lin et al., 2011), and a gene known to function in the GA-regulated processes of cell division and elongation, *PUX1* (At3G27310; *Plant Ubiquitin Regulatory X domain-containing Protein, 1*) (Rancour et al. 2004; Park et al., 2007; Supplemental Table S2). *PUX1* was selected for further characterization because it appeared to have the strongest interaction with *GID1b*, and because it was previously characterized as a negative regulator of plant growth and cell elongation (Rancour et al. 2004).

The *PUX1* cDNA clones recovered from the original yeast two-hybrid screen encoded two truncated proteins starting at amino acids 117 (T2) and 118 (T1) of PUX1, respectively (Supplemental Figure S1). These *PUX1* clones included all but the first 9–10 of the 73 amino acid UBX domain. The strength of protein interactions were examined using a yeast dilution series in the presence and absence of GA (Figure 1). Upon retest, both truncated *PUX1* clones (T1 and T2) displayed a GA-independent interaction with GID1b-Gal4bd (Figure 1A). The interaction of the full-length PUX1-Gal4ad was examined using both GID1b-Gal4db and GID1a-Gal4bd as a representative of the GID1a/c-type receptor (Figure 1, B and C). GA hormone appeared to enhance the interaction of PUX1-Gal4ad with GID1a-Gal4bd but not with GID1b-Gal4bd. This enhancement was not apparent when the interaction was confirmed using full-length PUX1-Gal4bd with GID1a-Gal4ad and GID1b-Gal4ad in bait and prey swap experiments (Supplemental Figure S2).

Loss of *PUX1* resulted in a constitutive GA response phenotype

If PUX1 plays a role in GA signaling via interaction with the GID1 GA receptors, then we would expect loss of *PUX1* function to alter GA responses including increased seed germination, cell elongation, and an earlier transition to flowering. *PUX1* was previously shown to be a negative regulator of plant cell elongation and growth based on the fact that two *pux1* T-DNA insertion alleles, *pux1-1* (intron 3 insertion) and *pux1-2* (exon 3 insertion), resulted in increased shoot and root elongation (Rancour et al., 2004). However, it was not known if *pux1* mutants affected other GA-stimulated processes such as germination and the transition to flowering, and whether these mutants exhibited altered GA sensitivity.

The effect of *pux1* mutants on seed germination was examined. GA stimulates and the GA biosynthesis inhibitor PAC inhibits seed germination in Arabidopsis (reviewed by Finkelstein et al., 2008). If *PUX1* is a negative regulator of germination, then we would expect mutations in this gene to result in increased germination capacity and increased resistance to PAC in germination. The *pux1-1* and *pux1-2* mutants were significantly more resistance to inhibition of seed germination by 1- and 0.5-μM PAC than wild-type (WT; Figure 2, A and B; Supplemental Figure S3). The *pux1-2* mutant appeared to be more resistant to PAC than *pux1-1*, suggesting that *pux1-2* results in a stronger constitutive GA response. It is possible that the T-DNA insertion in intron 3 in *pux1-1* has a weaker phenotype because it is sometimes spliced to produce a functional transcript causing this allele to function as a knockdown rather than knockout allele (Sandhu et al., 2013). The inhibition of germination by PAC was rescued by GA in WT Wassilewskija (Ws), *pux1-1*, and *pux1-2* seeds at 2 days of imbibition (Figure 2C).

Previous work showed that *pux1* mutants have longer shoots and roots than WT Ws, and that the longer roots were associated with increased root cell length in *pux1-2*

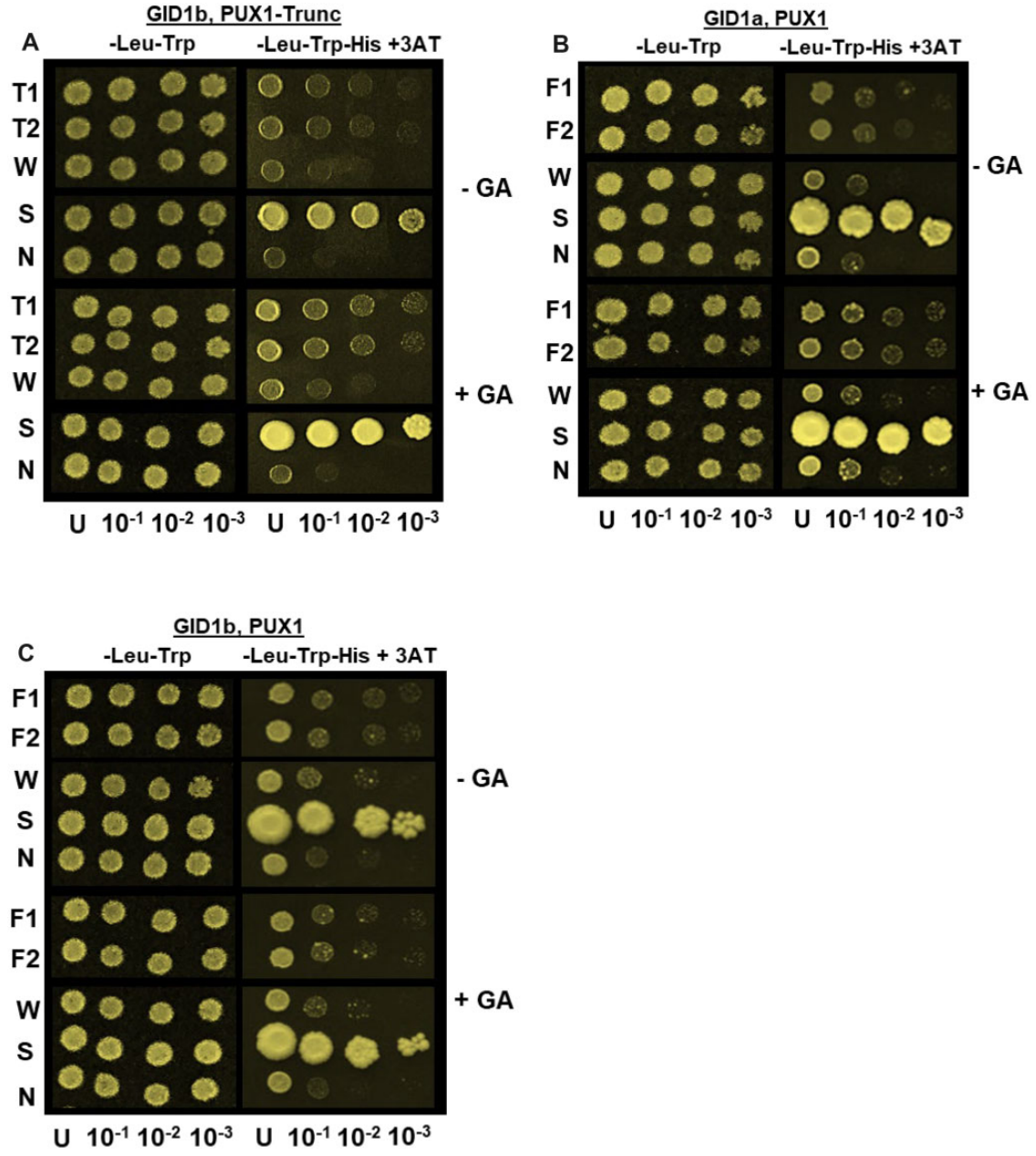

Figure 1 Detection of GID1–PUX1 protein interaction by yeast two-hybrid. Targeted yeast two-hybrid screens are shown between: (A) the GID1b bait and two independently recovered prey transformants, T1 and T2 containing truncated PUX1 proteins in the absence (−GA) or presence (+GA) of 10 μM GA_3. B and C, The full-length independent PUX1 prey transformants F1 and F2 in yeast lines carrying (B) the GID1a or (C) GID1b bait plasmids with or without 10 μM GA_3. Yeast samples were serially diluted and plated as undiluted (U) samples, and at dilutions of 1/10 (10^{-1}), 1/100 (10^{-2}), and 1/1,000 (10^{-3}) of U on synthetic dextrose media without leucine and tryptophan (−Leu−Trp), or without leucine, tryptophan, and histidine, and with 10-mM 3AT (−Leu−Trp−His + 3AT). Each screen included a weak interaction control (W), a strong interaction control (S), and a negative interaction control (N).

(Rancour et al., 2004). This phenotype is consistent both with increased GA signaling and with loss of PUX1 as a negative regulator of CDC48. If the *pux1* elongated-root phenotype results from constitutive GA signaling, root elongation should be more resistant to inhibition of GA biosynthesis by PAC (Karssen et al., 1989; Ariizumi et al., 2008). Treatment with 1-μM PAC resulted in a stronger decrease in Ws WT root length (46% of WT root length) than in *pux1-1* (59%) and *pux1-2* (57%) root length, respectively (Figure 3A; $P < 0.0001$). Thus, *pux1* mutants have decreased PAC sensitivity compared to WT, suggesting increased GA sensitivity. Because PAC inhibition of GA biosynthesis is not entirely specific, we examined the ability of 1-μM GA_4 treatment to recover root elongation on PAC. Root elongation on PAC is partly recovered by GA in all genotypes. WT root length on PAC + GA was similar to *pux1* mutant root length on PAC alone; GA treatment and *pux1* mutations rescued root length on PAC to a similar extent (Figure 3A). Based on

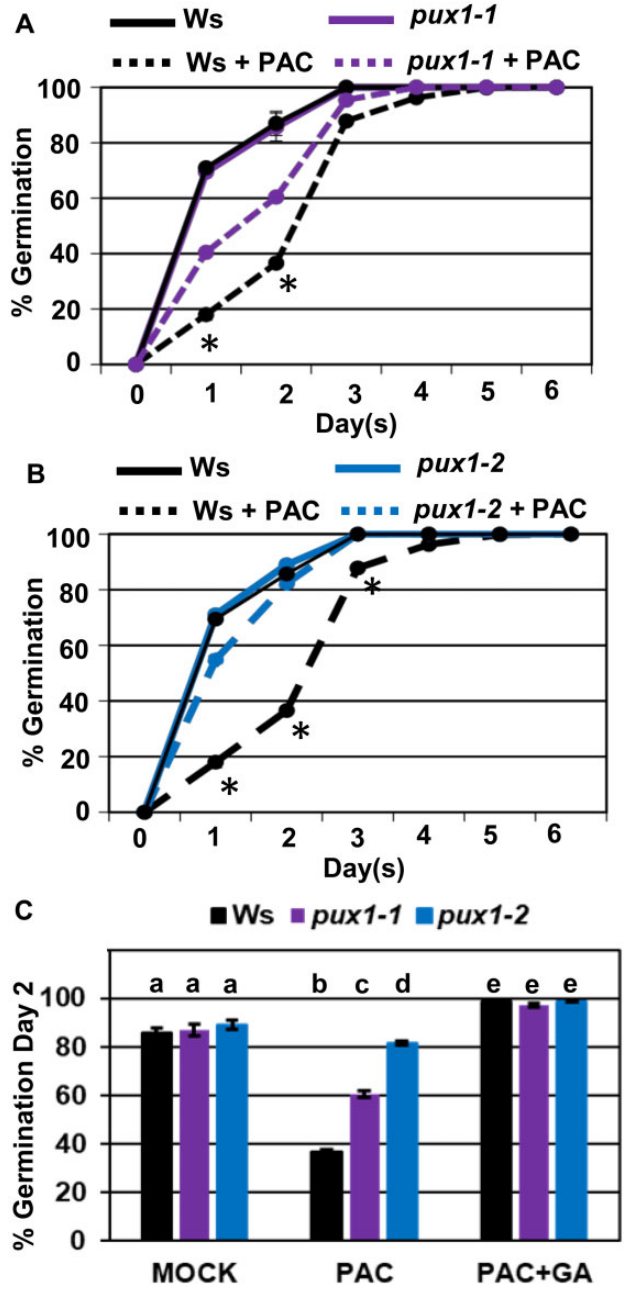

Figure 2 The *pux1* mutant seeds display decreased sensitivity to GA inhibitor PAC. Ws and *pux1* mutant seeds were imbibed at 4°C without or with 1-μM PAC for 24 h, washed 3 times with water and then plated on 0.5× MS agar plates without (A, B, and C) or with (C) 1-μM GA_4 to germinate in the light at 22°C. Germination was scored daily for 6 days until seeds stopped germinating. Percent germination across 6 days (A and B), or on Day 2 (C) is the average of three biological replicates, and $n = 100$. Statistical significance was determined by analysis of variance (ANOVA) using a Tukey's pairwise comparison, and $P < 0.05$ are indicated with an asterisk (A and B), or with letters to indicate significant categories (C).

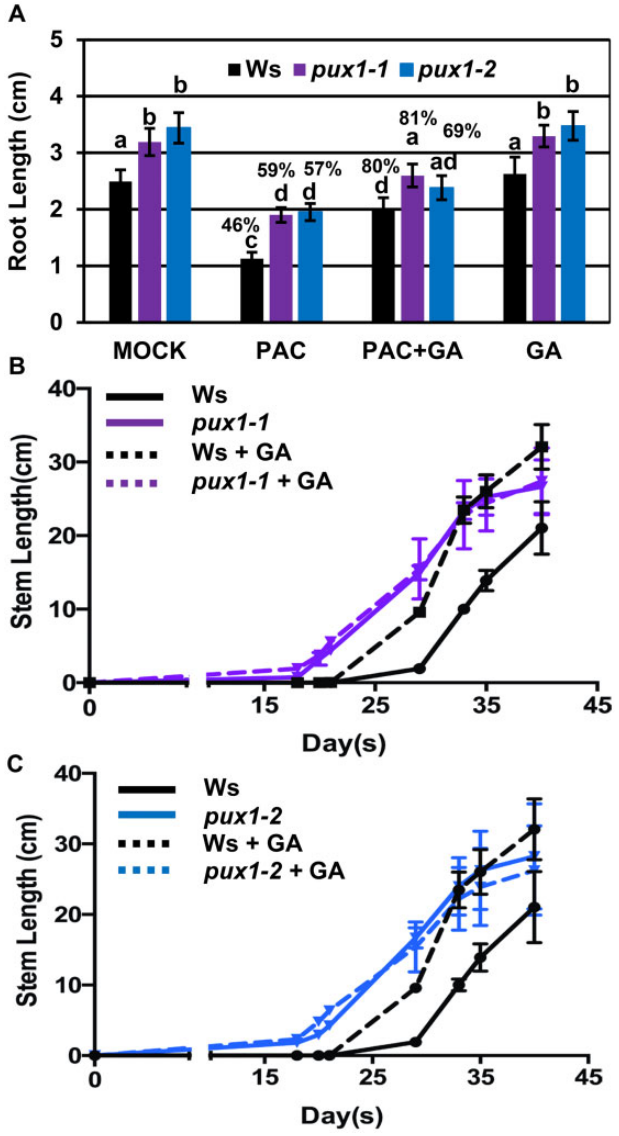

Figure 3 Decreased sensitivity of *pux1* mutants to PAC inhibition of root elongation and GA stimulation of stem elongation. A, Ws and *pux1* seedlings were grown on vertical 0.5× MS-agar plates without (mock), or with 1-μM PAC, 1-μM PAC plus 1-μM GA_4, or 1-μM GA_4 for 4 days. The average seedling root length was determined over three biological replicates, $n = 10$. Error bars = SD. Percent root growth of the PAC-treated or PAC + GA-treated versus mock-treated root length is given for each genotype. Letters indicate statistically different categories, P-value < 0.05 based on ANOVA with a Tukey's pairwise comparison. Stem length of Ws compared to (B) *pux1-1* and (C) *pux1-2* was measured from the soil surface to the shoot apex of GA-treated and mock-treated plants. Plants were sprayed with either 10-μM GA_3 or a mock treatment weekly starting at Day 8. Measurements were taken every other day. The average of 8–10 plants per genotype and treatment are shown, Error = SE, $n = 2$.

these results, it is likely that *pux1* has longer roots on PAC because GA signaling continues to function in the mutant.

Next, we examined the effect of *pux1* mutants on shoot elongation with and without weekly 10-μM GA_3 application. GA treatment resulted in no significant increase in *pux1-1* and *pux1-2* stem length relative to untreated mutant controls, whereas GA-treated WT stem length increased over the time course but never exceeded the *pux1* mutants (Figure 3, B and C; Table 1; Supplemental Figure S4). This lack of response to GA application does not

indicate GA insensitivity because *pux1-1* and *pux1-2* are not dwarves, rather it suggests that they reach maximum GA stimulation of stem elongation in the absence of hormone treatment.

GA signaling stimulates the transition to flowering in Arabidopsis (reviewed in Hauvermale et al., 2012). Consistent with increased GA signaling, *pux1-1* and *pux1-2* transitioned to flowering earlier than WT (Figure 4, A and B; Table 1). Ws WT seedlings flowered at the 14-leaf stage within 33 days after germination (DAG), whereas *pux1-1* and *pux1-2* flowered at the 5 and 6 leaf stage within 24 DAG (Figure 4, A and B; Supplemental Figure S5). Next, we examined whether 10-μM GA_3 application could speed the transition to flowering (Table 1). GA treatment caused Ws to transition to flowering faster, both in terms of number of leaves at bolting and in terms of DAG prior to flowering. The *pux1-1* and *pux1-2* mutants, however, showed no significant decrease in the number of leaves at flowering and a reduced response to GA based on DAG until flowering (Table 1). This suggests that the early flowering phenotype is due to constitutive GA signaling, such that GA treatment cannot further stimulate the transition to flowering. Thus, *PUX1* appears to negatively regulate GA response during seed germination, root and shoot elongation, and the transition to flowering.

pux1 mutants have altered expression of GA signaling and biosynthesis genes

Given that PUX1 functions as a negative regulator of GA signaling and interacts with the GID1 receptor, we examined the effects of *pux1* mutants on the mRNA and protein expression of GA biosynthesis and signaling genes (Dill et al., 2001; Griffiths et al., 2006; Hauvermale et al., 2012). GID1 protein levels were analyzed in total protein extracts from 4-day-old seedlings using an anti-GID1c antibody that recognizes all three GID1 proteins (Supplemental Table S3; Hauvermale et al., 2015). Overall GID1 protein levels were elevated in *pux1-1* compared to WT Ws seedlings (Figure 5, A and B). The increased GID1 levels in *pux1-1* may be one explanation for the "GA-overdose" phenotype observed in *pux1* mutants. The effect of the *pux1-1* mutant on *GID1a*, *GID1b*, and *GID1c* mRNA levels was examined by real-time reverse transcription-quantitative PCR (RT–qPCR) analysis (Figure 5C). Interestingly, *GID1a* mRNA levels were eight-fold higher in *pux1-1* than in WT Ws. In contrast, *GID1b* mRNA levels were 30% lower and *GID1c* mRNA levels unchanged in *pux1-1* versus WT (Figure 5C). Thus, *pux1-1* had differential effects on the expression of the *GID1a*, *GID1b*, and *GID1c* genes.

Next, we examined the effect of *pux1-1* on expression of the GA biosynthesis genes, *GA 20-oxidase 1* (*GA20ox1*) and *GA 3-oxidase 1* (*GA3ox1*), because previous work indicated that this gene family is subject to feedback downregulation by GA signaling (Rieu et al., 2008; Zentella et al., 2007). *GA20ox1* mRNA levels showed a 60% decrease whereas *GA3ox1* mRNA levels were not significantly different in *pux1-1* compared to WT (Figure 5C). Thus, it appeared that *GA20ox1* mRNA expression is subject to negative feedback regulation in response to the increased GA response phenotype of *pux1-1*.

GA binding to the GID1 receptor triggers degradation of DELLA proteins through the ubiquitin–proteasome pathway, thereby lifting DELLA repression of GA responses. Therefore, we examined the effects of *pux1-1* on DELLA RGA protein levels and on DELLA *RGA* and *GAI* mRNA levels. For RGA immunoblot analysis, seedlings were treated for 12 h with dimethyl Sulfoxide (DMSO) (mock treatment) or with the proteasome inhibitor MG132 (in DMSO) to determine if RGA protein levels are differentially affected by proteasomal

Table 1 Flowering time and leaf number of *pux1* mutants and Ws WT plants under exogenous GA application

Phenotype	No. of Rosette leaves	Total leaves	Bolting[a] (DAG)	Flowering[a] (DAG)
Ws	13.6 ± 1.6	17.0 ± 0.5	27	33
Ws + GA_3	9.4 ± 0.4*	13.0 ± 0.1*	22	26**
pux1-1	5.0 ± 0	7.5 ± 0.5	19	24
pux1-1 + GA_3	5.3 ± 0.3	7.6 ± 0.2	16	23
pux1-2	5.5 ± 0.5	8.0 ± 0.8	19	24
pux1-2 + GA_3	5.8 ± 0.3	8.0 ± 0.5	16	22

[a]Bolting and flowering time (DAG) were determined by measuring the number of total leaves present prior to the appearance of the inflorescence stem and first flower, respectively. Leaf number measurements were taken daily. SD represented by ±. Tukey's test was used to examine the statistical significance between the non-treated and GA-treated groups.
*$P < 0.05$, **$P < 0.01$.

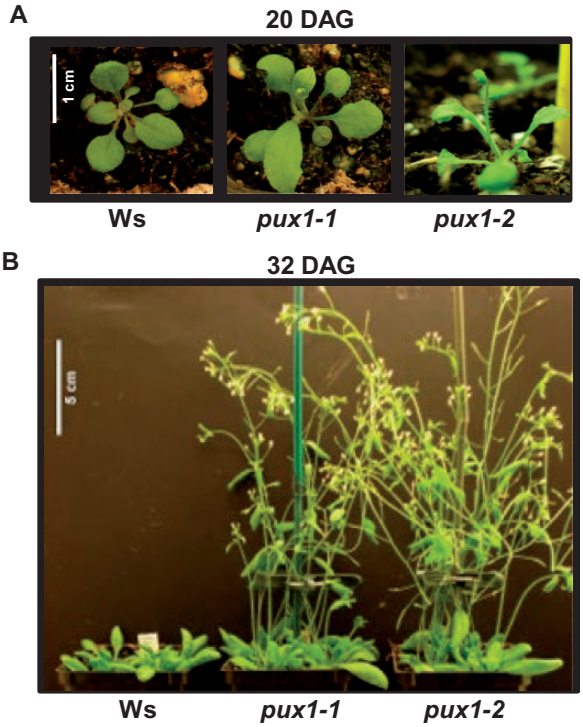

Figure 4 *pux1* mutants display an early flowering phenotype. A, Both *pux1-1* and *pux1-2* begin to bolt 20 DAG, and ~8–12 days earlier than Ws. B, A comparison between Ws and *pux1* mutants 32 days DAG shows both *pux1* mutants transitioned to flowering before Ws.

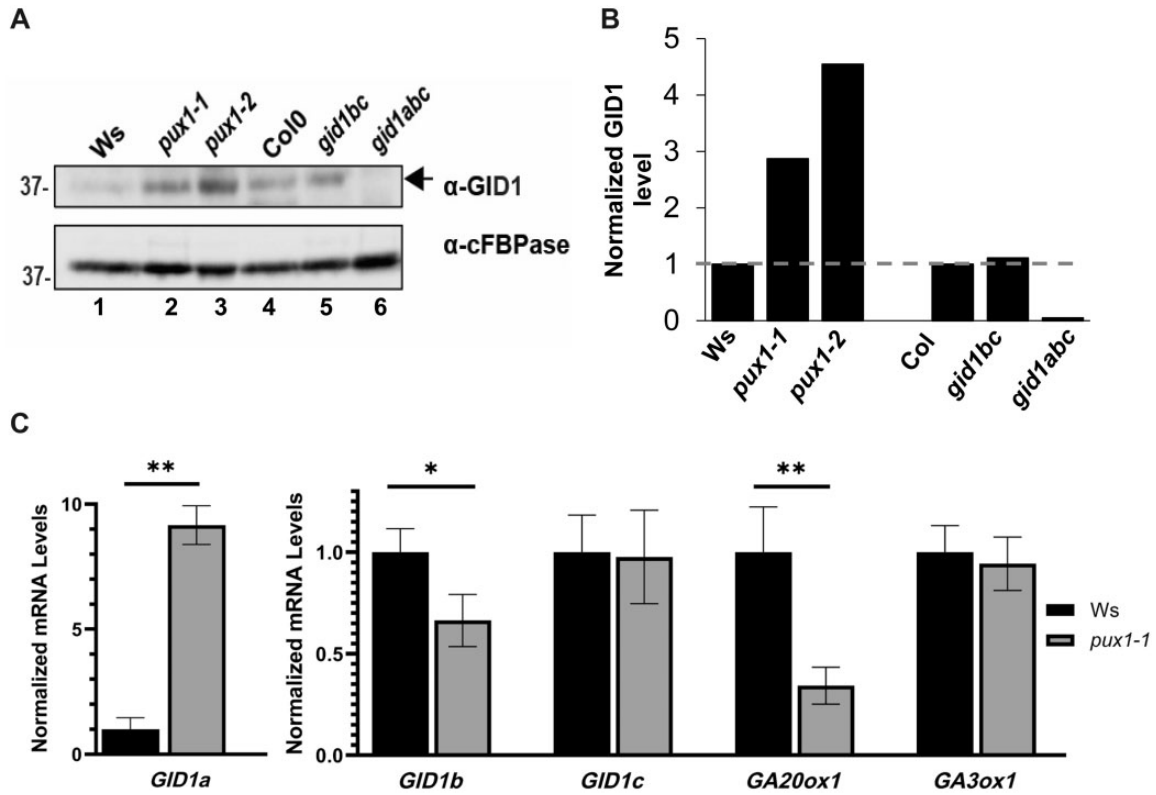

Figure 5 *pux1* mutants exhibit increased GID1 protein levels and decreased expression of *GA20ox1*. A, 30-μg total protein from 4-day-old Ws, *pux1-1*, *pux1-2*, Col-0, *gid1bc*, and *gid1abc* seedlings was fractionated by SDS–PAGE and analyzed by immunoblotting using anti-GID1 and anti-cytosolic FBPase (cFBPase; loading control) antibodies. B, Quantitative analysis of GID1 immunoblot signals in (A). Intensity of anti-GID1 relative to anti-cFBPase (loading control) immunoblot signals for each genotype were normalized to WT Ws for *pux1* mutants, Col-0 for *gid1* mutants. C, RT–qPCR analysis of *GID1a*, *GID1b*, *GID1c*, *GA20ox1*, and *GA3ox1* expression in 4-day-old *pux1-1* mutant and WT Ws seedlings. The mean normalized or relative expression is shown for three biological replicates for each individual gene. Error bars = SD. Statistical significance was determined by Student's *t* test, $^{*}P < 0.05$, $^{**}P < 0.01$.

degradation in *pux1-1* relative to WT. Following the mock treatment, RGA protein levels were 70% lower in *pux1-1* than in WT (Figure 6, A and B; Supplemental Figure S6). MG132 treatment resulted in increased RGA protein levels in both *pux1-1* and Ws relative to mock treatment. After MG132 treatment, there was no longer a significant difference between DELLA RGA levels in *pux1-1* versus WT. Moreover, MG132-treated *pux1-1* mutant DELLA RGA levels were similar to those in mock-treated WT. The partial rescue of RGA levels by MG132 treatment of *pux1-1* suggests that the decrease in *pux1-1* DELLA RGA levels may be partially due to increased proteasomal turnover of DELLA RGA in the mutant. There was insufficient resolution of the DELLAs RGA and GAI protein bands to enable independent quantitation of GAI protein levels (Supplemental Figure S6). As shown by RT-qPCR analysis, no significant difference in *RGA* and *GAI* transcript levels were detected in *pux1-1* relative to WT (Figure 6C), indicating that the decreased RGA protein levels in *pux1-1* likely result from posttranscriptional rather than transcriptional effects on RGA expression. Taken together, this suggests that the *pux1* "GA-overdose" phenotype may partly result from downregulation of DELLA protein accumulation.

GID1 and PUX1 proteins interact in vitro, and this interaction depends on the UBX domain

To examine if PUX1 and GID1 directly interact, in vitro binding assays were performed using purified glutathione S-transferase (GST)-tagged GID1b and GID1c and GST-free full-length PUX1 (Figure 7A). PUX1 copurified with GST-GID1b and GST-GID1c in the absence and presence of GA and did not interact with the GST negative control (Figure 7B).

To determine the region(s) of the PUX1 protein necessary for interaction with GID1, in vitro binding of GST-free PUX1 truncations (Figure 7A) to GST-GID1b, GST-GID1c, and GST alone were analyzed. Similar to full-length PUX1, PUX1 lacking the N-terminus (UBX-C) or C-terminus (N-UBX) bound to GST-GID1b and GST-GID1c in the presence or absence of GA (Figure 7C, upper two parts; Supplemental Figure S7). In contrast, the N-terminus of PUX1, lacking the UBX and C-terminal domains, did not bind to GST-GID1b, GST-GID1c, or GST (Figure 7C, middle). The PUX1 UBX domain resides between amino acids 101 and 181. However, to maintain solubility of the GST-UBX domain fusion protein, 13 and 10 amino acids that flank the N- and C-terminus of the UBX domain were included in the *Escherichia coli* expression

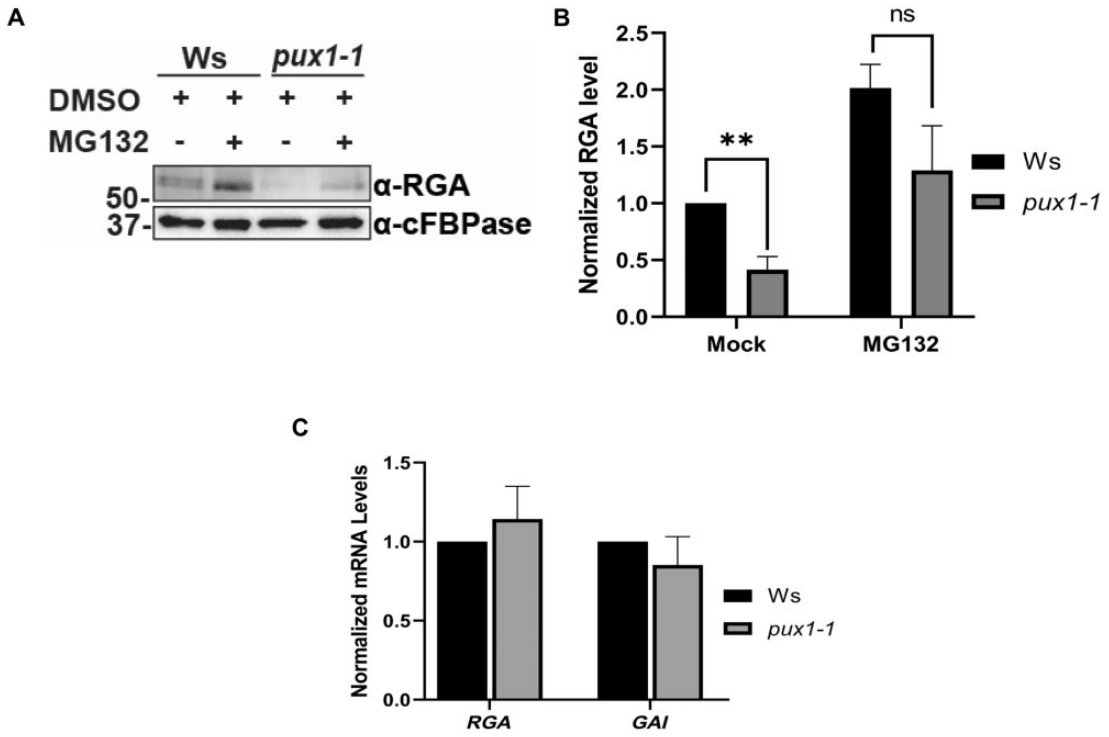

Figure 6 DELLA protein levels are decreased in *pux1-1* relative to WT. A, Immunoblot detection of the DELLA protein, RGA in total protein from Ws and *pux1-1* mutant 5-day-old seedlings treated with DMSO (mock) or MG132 + DMSO for 12 h. The cFBPase separated on the same gel was detected as a loading control. About 20 μg of total protein was loaded per lane. B, Quantitative analyses of the average anti-RGA immunoblot signal intensity in (A) and the three immunoblots shown in Supplemental Figure S7. Error bars represent SD for the mean of three biological replicates. Normalization was performed as in Figure 5. C, RT–qPCR analysis of *RGA* and *GAI* mRNA expression in the *pux1-1* mutant compared to WT Ws. Statistical significance was determined by Student's *t* test, ** indicates $P < 0.05$.

construct (13-UBX-10; Park et al., 2008). As shown in Figure 7C (bottom; Supplemental Figure S7), UBX (aa 88–191) bound to GST-GID1b and GST-GID1c compared to GST alone (Figure 7C, lane 1). Overall, these results demonstrate that the PUX1 UBX-domain is required and sufficient for the PUX1 interaction with GID1.

GID1 and PUX1 show a GA-independent interaction *in planta*

Co-immunoprecipitation assays were performed to determine whether PUX1 can interact with GID1 GA receptor proteins *in planta*, and whether this interaction depends upon GA hormone. Initial studies were performed in ungerminated, imbibed *ga1-3* seeds because a seed-specific cDNA library was used to identify PUX1 as a GID1b-interacting protein. To examine whether PUX1 co-immunoprecipitated with HA-tagged GID1 protein, total protein was extracted from *ga1-3 HA:GID1a* and *ga1-3 HA:GID1b* seeds imbibed without GA. PUX1 co-immunoprecipitated with HA:GID1a and HA:GID1b proteins using anti-HA magnetic beads (Figure 8A) regardless of whether or not GA hormone was added to the immunoprecipitation reaction. PUX1 also co-immunoprecipitated with HA:GID1a and HA:GID1b from 3-week-old Landsberg *erecta* (*Ler*) WT seedlings (Figure 8B) indicating that the GID1–PUX1 interaction can occur in rapidly growing seedlings capable of GA biosynthesis. The interaction between PUX1 and GID1 was specific as there was no PUX1 protein detected from co-immunoprecipitation experiments using *ga1-3 HA* seeds, or *Ler* HA seedlings (Supplemental Figure S8).

Since the GID1–PUX1 interaction was GA independent, we examined whether PUX1 protein accumulation depended upon GA. As previously reported in Ws WT, two proteins that migrated at ~38 kDa and ~34 kDa, referred to as PUX1-a and PUX1-b, were detected by immunoblot analysis using anti-PUX1 antibodies in both *Ler* WT and in the GA biosynthesis mutant *ga1-3* but were absent in *pux1-1* and *pux1-2* mutants (Figure 9A; Rancour et al., 2004). Quantitative analysis showed that the total levels of PUX1 protein were higher in *ga1-3* than *Ler* (Figure 9B). Furthermore, GA treatment resulted in a decrease of PUX1 accumulation in *ga1-3*, whereas PAC inhibition of GA biosynthesis in *Ler* and Ws increased the level of PUX1 (Figure 9B). Thus, PUX1 protein accumulation is negatively regulated by GA.

If GA signaling negatively regulates PUX1 accumulation, then the *gid1abc* triple mutant should show increased accumulation of PUX1 protein compared to Col WT. The *gid1abc* triple mutants and Col WT were treated with a mock treatment, PAC, and with PAC and GA together (Figure 9, C and D). Similar to *Ler* and Ws, Col WT showed increased accumulation of PUX1 with PAC treatment. When GA was added to the PAC treatment, the level of PUX1 decreased suggesting that the effect of PAC resulted from

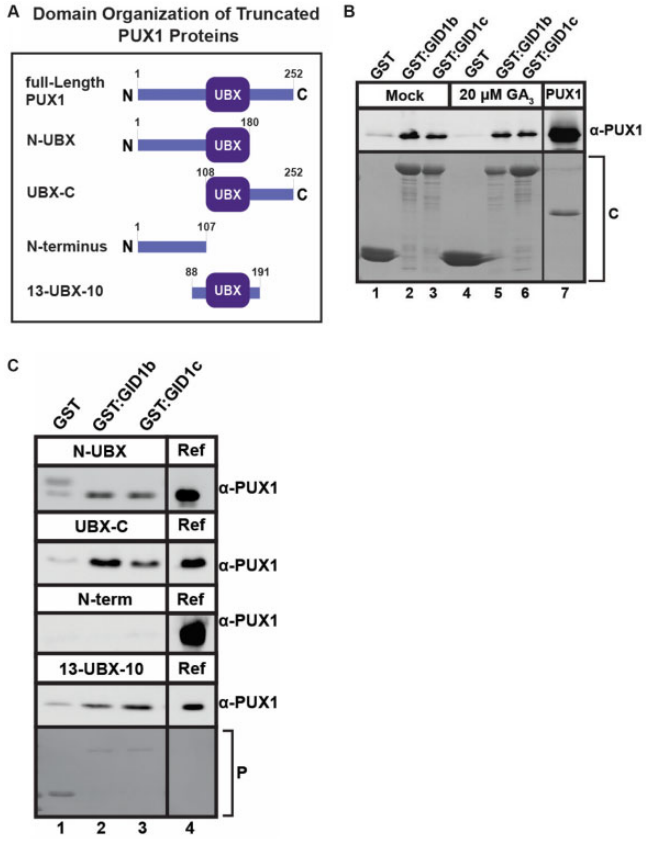

Figure 7 PUX1 binds GID1 in a GA-independent manner and requires its UBX domain for interaction. A, Protein domain organization of Arabidopsis full-length PUX1 and truncated constructs used to determine domains required for interaction with GST-tagged GID1 proteins. B, Purified GST (lanes 1 and 4) or GST-tagged GID1b,c (lanes 2–3 and 5–6) were incubated with tag-free full-length PUX1 in the absence of 20 μM GA_3. Purified PUX1 (lane 7) was used as a control. A Coomassie (C) stained gel was used to visualize input protein. C, In vitro analysis of truncated PUX1 binding to GST-GID1b and GST-GID1c. Purified GST (lane 1) or GST-GID1b,c (lanes 2 and 3) were incubated with tag-free N-UBX, UBX-C, 13-UBX-10, or the N-terminus of PUX1 in the absence of GA. The reference (Ref) control in lane 4 contains purified PUX1 truncation proteins. Ponceau Stain (P) was used to visualize input protein.

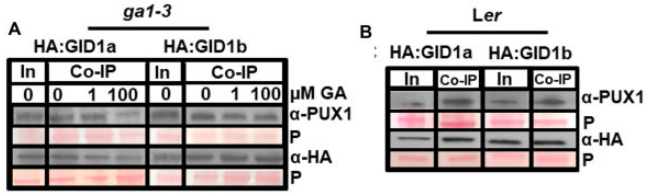

Figure 8 GID1 and PUX1 proteins interact *in planta*. A, PUX1 co-immunoprecipitation with HA:GID1 proteins extracted from *ga1-3 HA:GID1-OE* seeds, and (B) 4-day-old L*er HA:GID1-OE* seedlings. A total of 500 μg of seed protein extracts were incubated with α-HA magnetic beads with 0 μM, 1 μM, and 100 μM GA_4. Immunoblot analysis was performed with 60-μg protein input (In) and co-immunoprecipitated protein fractions. PUX1 protein was detected with anti-PUX1 primary antibody (1:5,000), and anti-rabbit horseradish peroxidase secondary antibody (Sigma; 1:10,000). Ponceau stained blots (P) were included to show protein loading.

decreased GA hormone levels. Interestingly, the *gid1abc* triple mutant showed a strong decrease instead of an increase in PUX1 protein levels. In contrast to Col WT, PAC and PAC plus GA treatment did not result in a substantial change in PUX1 protein levels in the *gid1abc* triple mutant. Taken together, these results indicate that GA and the GID1 receptors regulate PUX1 protein accumulation, but that this regulation is complex.

Co-fractionation studies of GID1, PUX1, and CDC48

Because the *pux1-1* mutant exhibited increased levels of GID1 protein, velocity sedimentation centrifugation experiments were performed to examine the effect of *PUX1* overexpression on GID1 and CDC48 protein *in vivo*. For these studies, we generated a stable transgenic Arabidopsis PSB-D cell line (Van Leene et al., 2011) expressing an N-terminal G-protein/Streptavidin-binding peptide (GS)-tagged PUX1 (GS-PUX1) construct. CDC48 fractionated as a hexameric complex (Figure 10, A and C, fractions 13–16; ~17.5 Svedberg units (S)) in protein extracts from untransformed PSB-D suspension cells whereas in extracts from GS-PUX1-overexpressing cells we detected both 17.5 S hexameric CDC48 (Figure 10, B and D, fractions 13–16) and ~5–8S nonhexamer-associated CDC48 subunits (Figure 10, B and D, fractions 5–7). This demonstrated that increasing levels of PUX1 promotes disassembly of the oligomeric CDC48 complex *in vivo* as previously demonstrated *in vitro* (Rancour et al., 2004; Park et al., 2007). In untransformed cells, GID1 co-fractionated with native PUX1 (Figure 10, A and C, fractions 5 and 6), but not with hexameric CDC48. In contrast, in cells overexpressing GS-tagged PUX1, we detected a shift in GID1 migration associated with co-fractionation of GS-PUX1, GID1, and CDC48 subunits at ~5–8S (Figure 10, B and D, fractions 5–7). Moreover, GS-PUX1 overexpression resulted in a reduction in the overall GID1 and native PUX1 protein levels (Figure 10, B and D). This suggests that PUX1 stimulates CDC48 disassembly, possibly promoting the formation of a PUX1–GID1–CDC48 complex.

While examining the effect of GS-PUX1 overexpression on CDC48 fractionation, we observed interesting differences in the velocity sedimentation fractionation profiles of CDC48 and PUX1 in protein extracts prepared from suspension-cultured cells versus protoplasts (Figure 10; Rancour et al., 2004; Park et al., 2007). Total protein extracts from protoplasts of the T87 Arabidopsis cell line showed the appearance of putative monomeric CDC48 (Supplemental Figure S9A; peak fractions 5–8) that were absent in protein extracts from whole (i.e. nonprotoplasted) T87 (Supplemental Figure S9B) and PSB-D (Figure 10A) cells. It may be that formation of protoplasts is a stress that induces PUX1-mediated CDC48 disassembly in a manner analogous to GS-PUX1 overexpression (Figure 10, B and D). Consistent with this, we observed a quantitative upward shift in the mobility of PUX1 such that all the PUX1 in protoplast

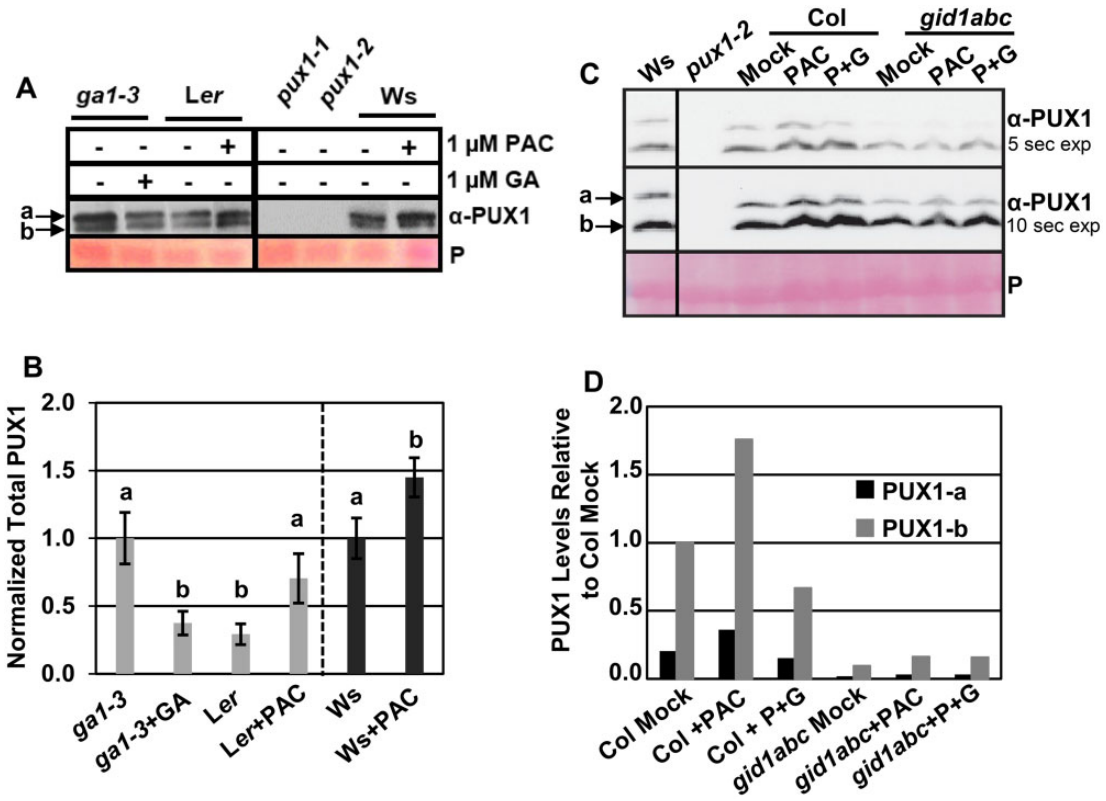

Figure 9 Regulation of PUX1 through GA signaling. A, PUX1 protein was detected by immunoblot analysis of 40-μg total protein extracted from *ga1-3* seeds with or without 1-μM GA_4 and L*er* and Ws seeds imbibed with and without 1-μM PAC. The two PUX1 protein isoforms, PUX1-a and PUX1-b, were not detected in *pux1* mutant seeds. B, Quantitation of total PUX1 protein in (A) and an additional independent experiment. PUX1 protein levels for GA-treated *ga1-3*, untreated L*er*, and PAC-treated Ler were normalized against untreated *ga1-3* (shaded bars). PUX1 protein levels for GA-treated Ws were normalized against untreated Ws (solid black bars). Statistical significance was determined by Student's *t*-test, letters indicate statistically significant categories with $P < 0.05$, and error bars = SD. C, Immunoblot detection of PUX1-a (38 kDa) and PUX1-b (34 kDa) in total protein from Ws, *pux1-2* mutant, Col, and *gid1abc* homozygous mutant seedlings treated with ethanol (mock), 1-μM PAC, or 1-μM PAC + 1 μM GA_4 (labeled P + G) for 12 h. About 20 μg of total protein was loaded per lane. A 5- and 10-s exposure of the anti-PUX1 immunoblots are shown. D, Quantitation of PUX1 isoforms in (C). PUX1 proteins were normalized against the Col mock treatment. Ponceau stained blots (P) were included for protein loading (A and C) and used to normalize protein abundance (B and D).

protein extracts co-fractionated in a ~5–8S complex with putative monomeric CDC48 (Rancour et al., 2004; Supplemental Figure S9A, peak fractions 5–8), whereas PUX1 from nonprotoplasted T87 (Supplemental Figure S9B, fractions 2–6) and PSB-D cell extracts (Figure 10A, fractions 1–6) fractionated in a peak of lower mobility that partially overlapped with putative monomeric CDC48.

Discussion

This paper provides evidence that the UBX domain-containing protein, PUX1, functions in GA hormone signaling. Mutations in GA signaling genes result in altered GA sensitivity and/or altered GA hormone accumulation. Mutations in *PUX1* result in increased GA sensitivity based on a decrease in response to PAC in seed germination and root elongation. The *pux1* mutants have all of the phenotypes expected of a GA hypersensitive mutant including increased germination capacity, increasing shoot and root elongation, and early flowering (Jacobsen and Olszewski, 1993). A yeast two-hybrid screen identified PUX1 as a GID1-interacting protein (Figure 1). Subsequent co-immunoprecipitation assays from plant extracts and in vitro binding studies with purified proteins demonstrated a GA-independent interaction between PUX1 and the GA receptors GID1a, GID1b, and GID1c (Figures 7 and 8). This interaction required the UBX domain of PUX1 (Figure 7). PUX1 accumulated at higher levels in the absence of GA, suggesting that GA negatively regulates PUX1 protein accumulation (Figure 9, C and D). Finally, *pux1* loss-of-function mutants have phenotypes consistent with increased GA signaling and sensitivity, suggesting that PUX1 is a negative regulator of GA responses.

The *pux1* mutants display accelerated flowering as well as shoot and root growth phenotypes similar to those previously described with loss of negative regulators of GA signaling, including DELLA and *spindly* (*spy*) mutants (Jacobsen and Olszewski, 1993; Swain et al., 2001; Shimada et al., 2006). The *spy* mutants were originally isolated based on the ability to germinate on 120 μM PAC. While the *pux1* mutants were less resistant to this GA biosynthesis inhibitor than *spy*

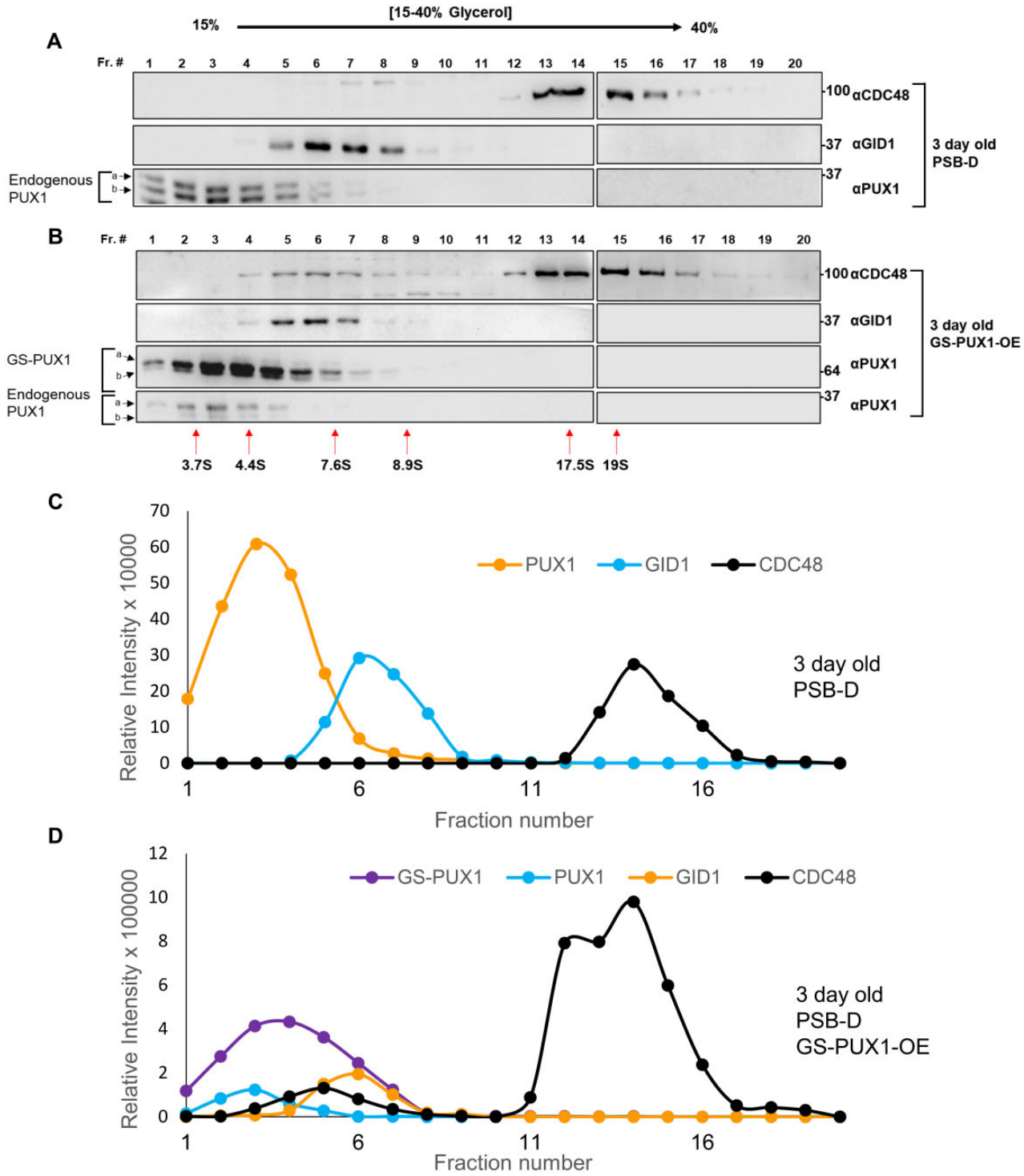

Figure 10 Velocity sedimentation analysis of GID1–PUX1–CDC48 interactions in Arabidopsis suspension-cultured cells. A, Immunoblot of glycerol gradient velocity sedimentation analysis and (C) signal intensity quantitation of native GID1, PUX1, and CDC48 from an untransformed 3-day-old Arabidopsis PSB-D cell line. B, Immunoblot of glycerol-gradient velocity sedimentation analysis and (D) signal intensity quantitation of GID1, PUX1, GS-PUX1, and CDC48 from 3-day-old GS-PUX1-OE Arabidopsis PSB-D cell line. Arrows indicate fractionation of molecular mass standards with their indicated Svedberg (S)-values. a, b indicates PUX1 isoforms.

mutants, they showed increased germination on 0.5- and 1.0-μM PAC compared to WT suggesting a reduced requirement for GA synthesis during germination (Figure 2; Supplemental Figure S3). Moreover, when bolting *pux1* plants were GA treated, no further stem elongation was observed, indicating that they had already reached maximum GA response (Figures 2–4; Table 1). Consistent with this "GA overdose" phenotype, the mRNA levels of the GA

biosynthesis gene, *GA20ox1*, were lower in the *pux1* mutant compared to WT (Figure 5). This suggests negative feedback regulation of GA biosynthesis in the GA hypersensitive *pux1* mutants (Griffiths et al., 2006; Rieu et al., 2008). The fact that *GA20ox1* responded, whereas *GA3ox1* did not, is not surprising given that *GA20ox* appeared to be more responsive to perturbations in GA signaling than *GA3ox* in transcriptome studies (Zentella et al., 2007).

Studies of GA signaling have focused on the negative regulation of DELLA repressors of GA responses by GA and GID1 (Ueguchi-Tanaka et al., 2005; Griffiths et al., 2006; Willige et al., 2007; Iuchi et al., 2007). GA binding to GID1 stimulates its association with DELLA proteins, leading to DELLA polyubiquitylation by SCF^{SLY1} and degradation via the 26S proteasome (McGinnis et al., 2003; Ueguchi-Tanaka et al., 2007; Murase et al., 2008; Shimada et al., 2008; Wang et al., 2009). Interestingly, the *pux1-1* mutation resulted in reduced DELLA protein accumulation, suggesting that *PUX1* negatively regulates GA responses by positively regulating DELLA protein levels (Figure 6). *PUX1* appears to regulate DELLA posttranscriptionally as *RGA* and *GAI* mRNA levels were unchanged in *pux1-1* (Figure 6C). It is possible that PUX1 interferes with proteasomal degradation of DELLA since treatment of *pux1-1* with the proteasomal inhibitor MG132 rescued DELLA RGA levels in the *pux1* mutant to levels similar to the untreated WT control (Figure 6A). Future work will need to examine if PUX1 participates in proteasomal and/or other proteolysis pathways leading to DELLA degradation. We cannot rule out a role for other degradation pathways as other members of the PUX protein family have been implicated in autophagy (Hussain et al., 2005; Wang et al., 2009; Gallois et al., 2013; Marshall et al., 2019; Huang et al., 2020).

Reduced DELLA protein levels in *pux1* mutants may result from the observed increase in GID1 receptor protein, which is associated with increased *GID1a* mRNA expression. The *pux1* mutant had no significant effect on *GID1c* mRNA levels, but was associated with decreased *GID1b* transcript levels (Figure 5). Because the GID1c antibody recognizes all three GID1 proteins as a single band, it is unclear whether only GID1a or all three GID1 proteins accumulate at higher levels in *pux1-1*. Future work will need to examine how mutations in *PUX1* result in altered *GID1* transcript levels and/or regulate the levels of GID1 posttranscriptionally. The notion that *PUX1* negatively regulates GID1 protein accumulation is supported by the observation that *PUX1* overexpression resulted in decreased GID1 levels (Figure 10). Based on this, one model is that PUX1 inhibits GA responses by negatively controlling GID1 activity thereby acting as a positive regulator of DELLA accumulation (Figure 11A). GA may govern this PUX1-dependent repression of GA signaling by negatively regulating PUX1 protein accumulation (Figure 9). Note that GA also directly regulates GID1 by stimulating GID1–GA–DELLA complex formation by triggering a change in GID1 protein conformation (Murase et al., 2008).

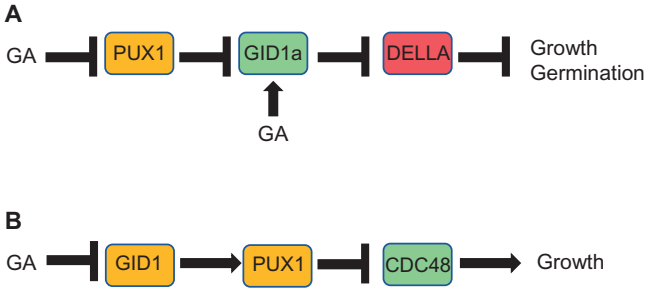

Figure 11 Two models for the role of PUX1 in GA hormone signaling. Based on mutant analysis, PUX1 is a negative regulator of *GID1a* mRNA and GID1 protein accumulation, as well as a positive regulator of DELLA RGA protein accumulation. A, One model is that PUX1 behaves as a negative regulator of growth and GA signaling because it positively regulates DELLA protein accumulation via negative regulation of GID1. B, A second model is that GA signaling stimulates growth via positive regulation of CDC48, a AAA + ATPase essential for cell division and homeostasis. In this case, GA negatively regulates PUX1, a negative regulator of CDC48. GID1 is required for control of PUX1 expression by PAC and GA. However, a complete null for *gid1a, b, c* leads to a severe reduction in PUX1 protein accumulation. This suggests that *GID1* genes are needed both for accumulation of PUX1 and for modulation of PUX1 accumulation/activity by GA when PUX1 is present.

Several lines of evidence raise the possibility that GID1 receptors may have specialized functions. Previous mutation analyses showed that *GID1b* can function as a negative regulator of seed germination and stem elongation under some conditions, whereas *GID1c* and *GID1a* generally behave as positive regulators (Griffiths et al., 2006; Ge and Steber, 2018; Hauvermale and Steber, 2020). It is interesting that *pux1-1* has opposite effects on *GID1a* and *GID1b* mRNA levels. This differential regulation is consistent with previous work showing that induced expression of a DELLA-deletion mutant (blocking GA signaling) had no effect on *GID1c* mRNA levels, but strongly increased *GID1b* and weakly increased *GID1a* mRNA levels (Zentella et al., 2007). Furthermore, the different GA receptors may have different effects on PUX1 regulation. While loss of GA biosynthesis due to PAC treatment or the *ga1-3* mutant resulted in increased PUX1 proteins levels, total loss of *GID1a*, *b*, and *c* function paradoxically resulted in decreased PUX1 protein levels (Figure 9). It is still possible that one or more of the GID1 receptors is needed for negative regulation of PUX1 by GA, because the *gid1abc* triple mutant is unresponsive to GA and PAC. Future work will need to examine whether different *gid1* mutants have differential effects on PUX1 and DELLA protein accumulation, and the ability of PUX1 to respond to PAC and GA treatment.

To date, the vast majority of GA signaling research has focused on DELLA proteins as nuclear-localized transcriptional regulators (reviewed by Hauvermale et al., 2012; Thomas et al., 2016). The model was that GA triggers DELLA destruction, lifting DELLA repression of GA responses via transcriptional activation (Zentella et al., 2007). However, recent research demonstrated a more complicated role for DELLAs

in transcriptional regulation and beyond (Locascio et al., 2013; Yoshida et al., 2014; Salanenka et al., 2018; Shanmugabalaji et al., 2018). For example, DELLAs sequester prefoldins in the nucleus. Upon GID1/GA-dependent DELLA destruction, prefoldins are released into the cytoplasm where they function in GA-stimulated microtubule reorientation and trafficking of the auxin efflux carrier PIN-FORMED 2 (McGinnis et al., 2003; Zentella et al., 2007; Locascio et al., 2013; Salanenka et al., 2018). This indicates that DELLA and/or GID1 may more directly stimulate cell growth. While DELLA proteins are nuclear localized, the GID1 receptors are present and function in both the nucleus and the cytoplasm (Ueguchi-Tanaka et al., 2005; Willige et al., 2007; Livne and Weiss, 2014). Likewise, both PUX1 and CDC48 proteins localize to both the cytoplasm and nucleus (Rancour et al., 2004; Park et al., 2008; Augustine et al., 2016). Future work will need to examine whether the GID1–PUX1 interaction occurs in the nucleus or cytoplasm. In addition, although GID1 and PUX1 interact, binding of PUX1 and GID1 is not dependent on GA and is thus not analogous to GID1 regulation of DELLA (Figures 7 and 8). Whether the GID1–PUX1 interaction allows GA and GID1 to control aspects of CDC48 signaling or allows CDC48 to regulate aspects of GA signaling remains to be determined (Figure 11B). We speculate that different GA receptors may have different effects on PUX1 and/or CDC48 regulation. The GID1–PUX1–CDC48 signaling pathway may function in this more nuanced aspect of GA signaling.

Our velocity sedimentation studies demonstrated that overexpression of GS–PUX1 in Arabidopsis cultured cells promotes disassembly of hexameric CDC48 resulting in co-fractionation of putative CDC48 monomers with GID1 (Figure 10), suggesting that CDC48 subunits may interact with both PUX1 and GID1. This is consistent with the observation that overexpression of the mammalian PUX1 homolog, Tethering containing UBX domain for GLUT4 (TUG)/Alveolar Soft Part Sarcoma Locus, results in disassembly of p97/CDC48 hexamers in human cultured cells (Orme and Bogan, 2012). Moreover, insulin hormone triggers TUG cleavage leading to increased glucose uptake by adipose tissue via transport of the GLUT4 receptor to the cell surface (Bogan et al., 2012). It is interesting that both PUX1 and TUG function in hormone signaling. Whereas insulin signals for glucose storage, GA triggers glucose mobilization in seeds. Thus, both pathways regulate energy storage/mobilization, suggesting a remarkable functional agreement across kingdoms.

These velocity sedimentation studies also revealed that GID1 protein fractionated with a larger sedimentation coefficient than expected for a globular protein with a molecular weight of 38–40 kDa, suggesting that GID1 is associated with other proteins in cultured Arabidopsis-cell lysates (Figure 10A, fractions 5–9; Figure 10B, fractions 4–9; Griffiths et al., 2006). Candidates for proteins in the GID1 complex include the GID1 interactors PUX1, DELLA, the GA receptor RING E3 ubiquitin ligase and Cryptochrome Circadian Regulator 1 (Nemoto et al., 2017; Xu et al., 2021; Zhong et al., 2021, Yan et al., 2021). Further work will also need to determine which of the 132 GID1 interactors identified by yeast two-hybrid have a functionally important GID1 interaction in plants (Supplemental Tables S1 and S2).

Based on data reported in Rancour et al. (2004) and the data presented in this article, we postulate that there is a regulatory connection between GID1, PUX1, and CDC48 proteins. An important function for AAA + ATPase CDC48 is the extraction and unfolding of ubiquitylated or sumoylated proteins from protein complexes during proteasomal degradation as well as nonproteolytic processes (Rosnoblet et al., 2021; Zhang et al., 2021). Both ubiquitylation and sumoylation pathways have been demonstrated to regulate GA signaling proteins including DELLA, GID1, and SLY1 (Conti et al., 2014; Kim et al., 2015; Campanaro et al., 2016; Nemoto et al., 2017; Blanco-Touriñán et al., 2020). Future work will need to examine if PUX1 and CDC48 regulate GID1 and DELLA activity and/or turnover via the ubiquitin–proteasome pathway. Indeed, loss of *PUX1* and *PUX1* overexpression increased and decreased GID1 protein levels, respectively (Figures 5, A and B and 10). PUX1 is an unusual UBX-containing CDC48 cofactor in that it exhibits the ability to promote the disassembly, and thereby, inactivation of hexameric CDC48 (Rancour et al., 2004; Park et al., 2007; Banchenko et al., 2019). Moreover, the PUX1 UBX domain required for CDC48 binding (Rancour et al., 2004; Park et al., 2007; Banchenko et al., 2019) is required for PUX1 interaction with GID1 (Figure 7). Thus, it is plausible that PUX1 binding to GID1 may serve to regulate PUX1-mediated disassembly of CDC48, thereby controlling the activity of this critical chaperone involved in diverse processes important for plant growth and development (Figure 11B; Park et al., 2008; Mérai et al., 2014). Given that GA signaling stimulates growth and that CDC48 has been shown to function in cell division, it is tempting to speculate that GA may regulate plant growth in part via stimulation of CDC48 function. Further studies are necessary to fully define the regions involved in GID1–PUX1–CDC48 protein–protein interactions, and to determine whether PUX1 functions as a GID1 adapter to facilitate and/or regulate its interaction with CDC48. CDC48 has been shown to function in organelle biogenesis including formation of the cell plate during cell division. If GA can positively regulate CDC48 by negatively regulating PUX1, potentially in a GID1-dependent manner, then it would provide an additional mechanism by which GA signaling stimulates cell division and expansion (Figure 11B). The notion that PUX1 and GID1 may have a function in GA signaling that is independent of DELLA protein destruction is consistent with the observation that *GID1* overexpression can partly rescue *sly1* mutant phenotypes without DELLA destruction (Ariizumi et al., 2008; Ueguchi-Tanaka et al., 2008; Hauvermale et al., 2014).

Since the initial isolation of GAs as the cause of increased stem elongation from "bakanae" disease nearly 100 years ago (Kurosawa, 1926; Takahashi et al., 1955; Geissman et al.,

1966), there have been significant advances in our understanding of the molecular mechanisms by which GA controls plant growth and development. Major milestones included the identification of genes required for GA biosynthesis and signal transduction, the identification of DELLA proteins as key negative regulators of GA response, the cloning of the GA hormone receptors, and the elucidation of GA-directed DELLA destruction by the ubiquitin–proteasome pathway (Silverstone et al., 1997; Peng et al., 1997; McGinnis et al., 2003; Itoh et al., 2003; Ueguchi-Tanaka et al., 2005; Griffiths et al., 2006; Nakajima et al., 2006; Hauvermale et al., 2012). This paper identified PUX1 as an element in GA signaling, opening a new area for investigation.

Materials and methods

Plant material and growth conditions

Arabidopsis thaliana lines included mutations in three ecotypes plus the corresponding WT. The *sly1-2*, *sly1-2 rga-24*, *sly1-2 gai-t6*, *ga1-3*, *ga1-3 HA*, *ga1-3 HA-GID1a*, *ga1-3 HA-GID1b*, L*er HA-GID1a*, and L*er HA-GID1b* lines were in L*er* (Steber et al., 1998; Ariizumi et al., 2008; Hauvermale et al., 2015). *Atcdc48a*, as well as the *gid1a-1*, *gid1b-1*, *gid1c-2* single, double, and triple mutants were in Columbia-0 (Col-0) (Willige et al., 2007; Park et al., 2008). The *pux1-1* and *pux1-2* mutants were in Ws (Rancour et al., 2004).

Seeds used for co-immunoprecipitation, germination, and root growth assays were sterilized with 10% (v/v) Bleach/0.01% (v/w) sodium dodecyl sulfate (SDS) for 10 min, rinsed with sterile water, and plated on 0.5× Murashige and Skoog (MS; Murashige and Skoog, 1962; Sigma-Aldrich, St. Louis, MO, USA) 5-mM 2-(N-morpholino)ethanesulfonic acid (MES) buffer pH 5.5 and 0.8% (v/w) agar (MS agar). Seeds utilized for stem and flowering measurements were sterilized with 70% (v/v) ethanol with 0.1% (v/v) Tween-20 for 5 min, 95% (v/v) ethanol for 1 min, moved to sterile filter paper to evaporate the ethanol and then plated on water-saturated filter paper.

Stock solutions were: (1) 10-mM PAC (Phytotechnology) suspended in methanol; (2) 10-mM gibberellin A3 (GA_3) and 10-mM gibberellin A4 (GA_4) (Sigma-Aldrich G7645, G7276) suspended in 70% (v/v) ethanol, and (3) 10-mM MG132 (Sigma) suspended in DMSO. For mock treatments, 70% (v/v) ethanol or methanol were diluted into water, MS agar, or MS solution to match the final solvent concentration in each treatment. Seeds were imbibed at 4°C for 3 days to cold stratify for even germination, and then transferred to a 22°C under 23 h fluorescent light (100 μmol m^{-2} s^{-1}) to germinate. Seedlings at the four leaf stage were transferred to soil and cultivated in a Conviron growth chamber at 22°C and with a 16-h day/8-h night photoperiod. The *ga1-3* and *ga1-3 HA:GID1* overexpression plants were sprayed weekly with 10 μM GA_3 until the green silique stage to rescue flowering and fertility.

Germination and root growth assays

For germination experiments, seeds were harvested at physiological maturity when siliques turned yellow, and then stored at room temperature for 2 months to ensure complete after-ripening, and then stored at −20°C to slow further after-ripening. Ws, *pux1-1*, and *pux1-2* seeds were imbibed with a mock treatment, or with 0.5 μM and 1-μM PAC with end-over-end mixing on a rotary mixer at 4°C for 24 h. Seeds were then rinsed with water, plated on MS agar, and germinated in the light at 22°C for 9 days (three replicates, $n = 100$). For root elongation experiments, seeds were germinated on MS agar, cold stratified for 3 days at 4°C, and then imbibed at 22°C for 2 days. Germinated seeds of the same age were moved to MS agar containing mock treatments, 1- μM PAC, 1-μM PAC plus 1-μM GA_4, or 1-μM GA_4, and were grown vertically under continuous light for 6 days (three replicates per treatment, $n = 10$). Ten seedling roots per replicate were photographed per genotype/treatment using a Sony Cyber-shot digital camera (DSC-W70), and root length was calculated using ImageJ software (Schneider et al., 2012).

Shoot elongation experiment

Seeds were sown in petri dishes on water-saturated filter paper and incubated for 3 days at 4°C to break dormancy. Seeds were subsequently incubated for 3 days at 22°C under constant light (T8 fluorescent bulb; 120 μmol m^{-2} s^{-1}) and then seedlings transplanted to soil. Plants were grown in growth chambers (Percival Scientific, Perry, IA, USA) under standard lighting conditions (16-h day/8-h night) at 22°C. Beginning at bolting (first appearance of buds), stem length (cm) was measured every other day, and plants were sprayed weekly with either exogenous 10-μM GA_3 or with a mock treatment ($n = 10$).

Measurement of flowering time

Plants were grown as described for the shoot elongation and flowering experiment (Table 1; Figure 3, B and C; Supplemental Figure S4). Differences in flowering time were measured based on: (1) the number of DAG until the first bud opened and (2) the number of rosette and cauline leaves present when the first bud opened (mean and standard deviation (SD), $n = 10$ plants) (Koornneef et al., 1991). For the long-day GA treatment, the treated plants were sprayed weekly with 10-μM GA_3 or mock treatment. Beginning at flowering, plant height was measured every other day from the soil level to the highest point of the plant. Each genotype was considered to have flowered/bolted when 50% of the biological replicates had the first flower open.

A second experiment characterized flowering phenotypes (Figure 4; Supplemental Figure S5). Ws WT and *pux1* mutant seedlings were plated on MS agar, cold stratified for 3 days at 4°C, and then transferred to 22°C under 23-h fluorescent light (100 μmol m^{-2} s^{-1}) to germinate. Seedlings were transplanted in soil at the four-leaf stage. Each pot contained four seedlings. Seedlings were grown in growth

chambers (Conviron) at a constant 22°C (16-h day/8-h night; metal halide lamps at 200 $\mu mol \cdot m^{-2} \cdot s^{-1}$). Leaf number, days to bolting, and flowering were recorded daily until Ws WT reached flowering. The time required for bolting/flowering of plants was measured as the DAG when 50% of all biological replicates for each genotype exhibited the first appearance of buds, respectively.

Yeast two-hybrid vector and library construction

The yeast two-hybrid screen for GID1 interactors used a cDNA library derived from dormant (2-weeks after-ripened) and less dormant (2-months after-ripened) L*er* WT and *sly1-2* seeds. After-ripening time points were chosen to obtain both fully dormant and partly after-ripened *sly1-2* seeds at 2 weeks and 2-months after-ripening, respectively (Supplemental Figure S10; Ariizumi et al., 2013; Nelson and Steber, 2017). Because 2-months after-ripening partially rescued *sly1-2* germination/GA signaling, these seeds were expected to include transcripts needed for the GA signaling that occurs without DELLA destruction. Seeds were plated on 0.5× MS-saturated filter paper and incubated at 4°C for 4 days, and then moved to 22°C in the light for 2 days. Total RNA was isolated from combined seeds (dry and imbibed, dormant and after-ripened L*er* and *sly1-2*) using the RNAqueous kit (Ambion, Austin, TX, USA) (Kushiro et al., 2004). mRNA was isolated using the PolyATtract mRNA Isolation System (Promega, Madison, WI, USA). The CloneMiner cDNA Library Construction Kit was used to construct a three-frame cDNA library from 1 μg of mRNA (Invitrogen Waltham, MA, USA). The primary entry library was amplified once resulting in a final titer of 3.21×10^{12} colonies. An aliquot of the amplified entry library (6.0×10^{7} colonies) was recombined into the ProQuest pDEST22 yeast two-hybrid prey vector (Invitrogen). Full-length *GID1a*, *GID1b*, and *PUX1* open-reading frames (Rancour et al., 2004; Ariizumi et al., 2008) were PCR amplified using gene-specific primers (Supplemental Table S4), cloned into the TOPOGW8 gateway entry vector (Invitrogen), and recombined into the ProQuest pDEST32 prey (*LEU2* selection) and pDEST22 bait (*TRP1* selection) vectors to generate in-frame GAL4 DNA-binding domain (Gal4db) GAL4 transcriptional activation (Gal4ad) domain fusions, respectively.

Yeast two-hybrid screen

GID1b-interacting proteins were identified by yeast two-hybrid screen (Proquest Two Hybrid System, Invitrogen; Fields and Song, 1989; Walhout and Vidal, 2001). The *GID1b* bait and cDNA library prey plasmids were transformed into MAV203 yeast by the lithium acetate method (Gietz and Woods, 2002). Protein interactions resulted in expression of *GAL4* promoter fusions to *HIS3* and *URA3*, detected based on growth on synthetic dextrose media lacking histidine and uracil. Top candidates were detected based on growth on media lacking histidine but containing 10-mM 3-amino-1,2,4-triazole (3AT; Sigma-Aldrich) and then were confirmed based on growth on media lacking uracil (Supplemental Table S2). Directed yeast two-hybrid assays of interaction candidates were performed on synthetic dextrose media without leucine, tryptophan, and histidine, and in the presence of 10-mM 3AT, and without or with 10-μM GA_3. Plasmids, pDEST32, and pDEST22 were used as a negative interaction control, the pEXP32/Krev1 bait with pEXP22/RalGDS-*wt* prey plasmid were used as a strong interaction control, and the pEXP32/Krev1 bait with pEXP22/RalGDS-m1 prey plasmid were used as a weak interaction control (Herrmann et al., 1996; Serebriiskii et al., 1999). Full-length PUX1 interactions with GID1b and GID1a were confirmed with PUX1 as both the bait and the prey (Supplemental Figure S2).

GID1 and PUX1 immunoblot, co-immunoprecipitation, and quantitative analyses

Antibodies used in study can be found in Supplemental Table S3. Seeds were after-ripened for 2 months at room temperature to allow dormancy loss. For immunoblot analysis, seeds were incubated in the light for 24 h at 22°C with and without 1-μM GA_4, or with and without 1-μM PAC. For co-immunoprecipitation experiments, proteins were extracted from *ga1-3 HA* and *HA-GID1a/b* seeds that were stratified for 3 days at 4°C in the dark to obtain synchronous germination, then incubated for 2 days at 22°C in the light (Ariizumi et al., 2008). For L*er HA-GID1a/b* experiments, extracts were prepared from 3-week-old seedlings. Seeds and seedlings were ground in liquid nitrogen and mixed with extraction buffer (50-mM potassium phosphate buffer pH 7.0/1× protease inhibitor cocktail (Sigma-Aldrich)). Protein concentrations were determined by the Quickstart Bradford assay (BioRad, Hercules, CA, USA) and 40 μg of total protein was reserved from each sample for immunoblot analysis and 60 μg for input control for co-immunoprecipitation experiments.

For analysis of PUX1 protein levels in Col, seedlings were grown on MS agar in the light 5 days at 22°C. For analysis of PUX1 protein levels in *gid1abc* seedlings, homozygous triple mutants were recovered from a segregating *GID1a/gid1a gid1b/gid1b gid1c/gid1c* line by identifying the 25% ungerminated seeds, then nicking the seed coat to stimulate germination (Willige et al., 2007; Ge and Steber, 2018; Hauvermale and Steber, 2020) and grown on MS agar in the light 5 days at 22°C. Five-day-old Col and *gid1abc* mutant seedlings were then moved to MS agar containing either mock treatment, 1-μM PAC, or 1-μM PAC plus 1-μM GA_4 (P + G) for 12 h. For analysis of GID1 protein levels in WS, Col, *pux1* mutant, *gid1bc* double mutant, and *gid1abc* triple were grown for 4 days on MS agar. For protein analysis, all seedlings were ground in liquid nitrogen. About 50–100 μL of homogenized tissue was resuspended in 25–50 μL of 2× SDS–PAGE (SDS-polyacrylamide gel electrophoresis) sample buffer (Laemmli, 1970), heated for 5 min at 95°C and centrifuged at 16,000 *g* for 5 min at room temperature. Soluble supernatant was collected, and protein concentration determined using Pierce 660-nm Protein Assay with Ionic Detergent Compatibility Reagent (Thermo Scientific Waltham, MA, USA). About 20

or 30 μg of total protein for each sample were separated on a 12.5% SDS–PAGE and transferred to nitrocellulose membrane by electroblotting (Hoefer TE22) at 300 mA for 2.5 h. Membranes were incubated at room temperature with blocking buffer (4% (w/v) milk in Tris-buffered saline solution (20-mM Tris, 150-mM NaCl) including 0.1% (v/v) Tween-20; TBS-T). Blots were incubated with anti-PUX1 (Rancour et al., 2004) or anti-GID1c antibodies in blocking buffer overnight at 4°C. Membranes were washed 3 times with TBS-T for 15 min, then incubated for 1 h at room temperature with anti-rabbit IgG-horseradish peroxidase secondary antibodies (Invitrogen). Protein detection was performed using an enhanced chemiluminescent system according to the manufacturer's protocol (SuperSignal ECL; Thermo Scientific). Immunoblots were imaged using the iBright C1000 Imaging System (Invitrogen) and quantitation of protein bands was performed using Photoshop. PUX1 and GID1 protein intensity were normalized to the Ponceau controls (Figures 5, 6, and 9, C and D). Figure legends indicate the number of replications analyzed for each experiment.

For co-immunoprecipitation, total seed protein extracts (500-μg reaction^{-1}) were treated with 0, 1, and 100-μM GA_4 and incubated with anti-HA-tag mAb magnetic beads (MBL International, Woburn, MA, USA) at 4°C overnight with gentle agitation (Figure 8). Beads were washed 3 times with 1-mL extraction buffer with or without GA_4 as indicated and resuspended in 15 μL of extraction buffer with 15 μL of 2× loading buffer (BioRad). For protein blot experiments, protein samples were denatured by heating at 95°C for 5 min, fractionated on precast "Any kD" TGX gels, and blotted to PVDF membranes using a semi-dry Turbo transblotter at 25 V for 14 min (BioRad) (Figures 8 and 9, A and B). Membranes were rinsed with Tris-buffered saline buffer (20-mM Tris, 150-mM NaCl, 0.1%) including 0.1% (v/v) Tween-20 (TBS-T) and incubated at room temperature for 30 min with blocking solution (0.2% (v/v) ECL block in TBS-T; GE Healthcare, Chicago, IL, USA). Blots were rinsed in TBS-T and shaken with either anti-PUX1 antibody for 2 h at room temperature, or anti-HA antibody for 1 h at room temperature. Membranes were washed with TBS-T, and then incubated for 1 h at room temperature with anti-rabbit IgG-horseradish peroxidase. Protein detection was performed using an enhanced chemiluminescence system according to the manufacturer's protocol (ECL advance; GE Healthcare). Immunoblots were visualized with a ChemiDoc imaging system (BioRad), and relative protein band intensities normalized against a Ponceau-stained control. Fold change differences in protein band intensity were determined using Image Lab software version 6.0.1 (BioRad) (Figure 9, A and B). Figure legend indicates the number of replications analyzed for each experiment.

Quantitative analysis of DELLA protein levels

Antibodies used in study can be found in Supplemental Table S3. Ws WT and *pux1* mutant seedlings were grown on MS agar in the light 5 days at 22°C. Seedlings were then moved to MS-agar containing either mock treatment or 50-μM MG132 for 12 h. For protein analysis, all seedlings were ground in liquid nitrogen. Homogenized tissue of 100 μL was resuspended in 50 μL of 2× SDS–PAGE sample buffer, heated for 5 min at 95°C and centrifuged at 16,000 *g* for 5 min at room temperature. Soluble supernatant was collected, and protein concentration determined using Pierce 660-nm Protein Assay with Ionic Detergent Compatibility Reagent (Thermo Scientific). Twenty micrograms of protein was separated on a 12.5% SDS–PAGE gel and immunoblotted as described above with anti-GID1, anti-RGA, and anti-cFBPase.

GST-binding studies

GST and GST-tagged GID1 proteins expressed in *E. coli* were affinity purified (Griffiths et al., 2006; Ariizumi et al., 2008). Affinity purified full-length and truncated PUX1 proteins were prepared and treated to remove the GST-tag (Park et al., 2007). GST or GST-tagged GID1 proteins were incubated with either tag-free full-length PUX1 (at a molar ratio of 1:1) or tag-free truncated PUX1 in 100 μL of binding buffer (20-mM HEPES/KOH, pH 7.4, 150-mM KCl, 1-mM $MgCl_2$, 2-mM β-mercaptoethanol, 0.1% (v/v) NP-40) without GA or with 20-μM GA_3. Reactions were incubated on ice for 30 min followed by affinity isolation using Glutathione-Sepharose resin (Bioworld). Bound complexes were washed 5 times with binding buffer and eluted with 50-mM Tris–HCl, pH 8.1, 150-mM NaCl, 10-mM glutathione. Protein samples were fractionated by 12.5% SDS–PAGE and immunoblotted as described above using anti-PUX1 antibodies.

Glycerol-gradient velocity sedimentation analysis

Arabidopsis T87 and PSB-D suspension-cultured cells were maintained as described in Axelos et al. (1992), Kang et al. (2001), and Van Leene et al. (2011). Cytosolic extracts from 3-day-old suspension-cultured cells were generated as in Mayers et al. (2017) with the following modifications. Cells were washed in lysis buffer (20-mM HEPES/KOH, pH 7.4, 150-mM KCl, 1-mM $MgCl_2$, 2-mM β-mercaptoethanol, 1-mM DTT, 0.01-mg mL^{-1} E-64 + Protease inhibitor cocktails (PICD and PICW described in Rancour et al., 2002) 3 times, lysed under pressure with a N_2 cell disruptor, and then centrifuged at 106,000 *g* for 20 min at 4°C using a TLA100.3 rotor (Beckman Coulter, Brea, CA, USA). For preparation of T87 protoplast cytosolic extracts, 3-day-old T87 cells were protoplasted and lysed as in Kang et al. (2001) and Rancour et al. (2004). Cytosolic extracts were layered on top of a 15%–40% (v/v) glycerol gradient and centrifuged at 120,000 *g* for 16 h at 4°C in an SW 50.1 rotor (Beckman Coulter). Collected fractions were analyzed by immunoblot. Protein sedimentation standards including ovalbumin (44 kDa, 3.7S, Sigma-Aldrich), BSA (66 kDa, 4.4S, Sigma-Aldrich), yeast alcohol dehydrogenase (37.5 kDa × 4, 7.6S, Sigma-Aldrich), sweet potato beta-amylase (50 kDa × 4, 8.9S, Sigma-Aldrich), catalase (60 kDa, Sigma-Aldrich), apoferritin (24 kDa × 20, 17.7S, MP Biomedicals, Santa Ana, CA, USA), and thyroglobulin (334 kDa, 19S, Sigma-Aldrich) were determined on parallel

15%–40% (v/v) glycerol gradients. The fractionation profile of the protein standards was analyzed by SDS–PAGE followed by staining with Coomassie blue and densitometry performed using an ImageQuant LAS4010 digital imaging system (GE Healthcare Life Sciences) to generate standard curves from which experimental S-values were determined as an estimate of native molecular weight.

RT–qPCR

Plant total RNA was extracted from 4-day-old Arabidopsis seedlings using the RNeasy Plant Mini Kit (Qiagen, MD) with DNAse I treatment (Life Technologies) to remove genomic DNA. cDNA was synthesized using SuperScript III Reverse Transcriptase (Invitrogen). RT–qPCR reactions were performed using SYBR Green Master mix (Roche, Basel, Switzerland), cDNA template, and 0.3 μM of each gene-specific primer (Supplemental Figure S4). *TUB5* and *UBC18* were used as internal controls for normalizing gene expression. A three-step PCR cycle was performed using a 7500 Fast Real Time PCR system (Applied Biosystems) to determine the cycle threshold (C_T) and relative transcript levels calculated using the delta–delta C_T method (Livak and Schmittgen, 2001).

Accession numbers

Arabidopsis gene and protein sequence data can be found in the Arabidopsis Information Resource (https://www.arabidopsis.org/): *CDC48a* (AT3G09840), *GAI* (AT1G14920), *GA20ox1* (AT4G25420), *GA3ox1* (AT1G15550), *GID1a* (AT3G05120), *GID1b* (AT3G63010), *GID1c* (AT5G27320), *RGA* (AT2G01570), *PUX1* (AT3G27310), *SLY1* (AT4G24210), *cFBPase* (AT1G43670), *UBC18* (AT5G42990), and *TUB5* (AT1G20010).

Supplemental data

The following materials are available in the online version of this article.

Supplemental Figure S1. Amino acid sequence alignment of PUX1 and truncated transformants T1 and T2 isolated from the yeast two-hybrid screen.

Supplemental Figure S2. Detection of in vivo interactions between GID1 and PUX1 proteins in bait prey swaps.

Supplemental Figure S3. Mutant *pux1* seeds display decreased sensitivity to GA inhibitor paclobutrazol.

Supplemental Figure S4. Loss-of-function *pux1* mutants are nonresponsive to exogenous GA.

Supplemental Figure S5. At 32 DAG, Ws WT has just transitioned to flowering.

Supplemental Figure S6. Immunoblot analysis of DELLA protein levels in *pux1-1* and WT seedlings.

Supplemental Figure S7. Binding of the PUX1 UBX domain to GID1 is not affected by the presence of GA.

Supplemental Figure S8. Validation of anti-HA antibody specificity: anti-HA antibodies did not immunoprecipitate PUX1 protein.

Supplemental Figure S9. Differences in the velocity sedimentation profile of PUX1 and CDC48a in cell extracts from T87 protoplasts and T87 suspension-cultured cells.

Supplemental Figure S10. Germination efficiency of dormant and after-ripened L*er* WT and *sly1-2* seeds used to generate the yeast two-hybrid cDNA library.

Supplemental Table S1. Yeast two-hybrid screen summary.

Supplemental Table S2. List of GID1b interactors.

Supplemental Table S3. Antibodies used in this study.

Supplemental Table S4. Primers used in this study.

Acknowledgments

The authors would like to thank Drs. J. Browse, K. Gill, H. Hellmann, R. Reeves at Washington State University, and Drs. H. Holden, M. Otegui, R. Amasino, at the University of Wisconsin- Madison for their helpful suggestions on manuscript preparation. We are also grateful to W. Spivia and G. Schimdt (Verona Area High School) for technical assistance. Thanks are due to members of the Steber and Bednarek lab for comments on the research and manuscript.

Funding

This work was supported by grants to S.Y.B. from the USDA National Institute of Food and Agriculture, Hatch project (No. WIS01846 and WIS03046), C.M.S. National Science Foundation (Award #085098), and an award to J.J.C. from the National Science Foundation Graduate Research Fellowship Program (DGE-1256259)

Conflict of interest statement. None declared.

References

Ariizumi T, Hauvermale AL, Nelson SK, Hanada A, Yamaguchi S, Steber CM (2013) Lifting DELLA repression of Arabidopsis seed germination by nonproteolytic gibberellin signaling. Plant Physiol **16**: 2125–2139

Ariizumi T, Murase K, Sun TP, Steber CM (2008) Proteolysis-independent downregulation of DELLA repression in Arabidopsis by the gibberellin receptor GIBBERELLIN INSENSITIVE DWARF1. Plant Cell **20**: 2447–2459

Ariizumi T, Steber CM (2007) Seed germination of GA-insensitive *sleepy1* mutants does not require RGL2 protein disappearance in Arabidopsis. Plant Cell **19**: 791–804

Augustine RC, York SL, Rytz TC, Vierstra RD (2016) Defining the SUMO system in Maize: SUMOylation is up-regulated during endosperm development and rapidly induced by stress. Plant Physiol **171**: 2191–2210

Axelos M, Curie C, Mazzolini L, Bardet C, Lescure B (1992) A protocol for transient gene-expression in *Arabidopsis thaliana* protoplasts isolated from cell-suspension cultures. Plant Physiol Biochem **30**: 123–128

Banchenko S, Arumughan A, Petrović S, Schwefel D, Wanker EE, Roske Y, Heinemann U (2019) Common mode of remodeling AAA ATPases p97/CDC48 by their disassembling cofactors ASPL/PUX1. Structure **27**: 1830–1841.e3

Blanco-Touriñán N, Serrano-Mislata A, Alabadí D (2020) Regulation of DELLA proteins by post-translational modifications. Plant Cell Physiol **61**: 1891–1901

Bogan JS, Rubin BR, Yu C, Löffler MG, Orme CM, Belman JP, McNally LJ, Mingming H, Cresswell JA (2012) Endoproteolytic cleavage of TUG protein regulates GLUT4 glucose transporter translocation. J Biol Chem **287**: 23932–23947

Campanaro A, Battaglia R, Galbiati M, Sadanandom A, Tonelli C, Conti L (2016) SUMO proteases OTS1 and 2 control filament elongation through a DELLA-dependent mechanism. Plant Reprod **29**: 287–290

Conti L, Nelis S, Zhang C, Woodcock A, Swarup R, Galbiati M, Tonelli C, Napier R, Hedden P, Bennett M, et al. (2014) Small ubiquitin-like modifier protein SUMO enables plants to control growth independently of the phytohormone gibberellin. Dev Cell **28**: 102–110

Derkx MPM, Vermeer E, Karssen CM (1994) Gibberellins in seeds of *Arabidopsis thaliana*: biological activities, identification and effects of light and chilling on endogenous levels. Plant Growth Regul **15**: 223–234

Dill A, Jung HS, Sun TP (2001) The DELLA motif is essential for gibberellin-induced degradation of RGA. Proc Natl Acad Sci USA **98**: 14162–14167

Fields S, Song OK (1989) A novel genetic system to detect protein–protein interactions. Nature **340**: 245–246

Finkelstein R, Reeves W, Ariizumi T, Steber C (2008) Molecular aspects of seed dormancy. Ann Rev Plant Biol **59**: 387–415

Foley ME, Fennimore SA (1998) Genetic basis for seed dormancy. Seed Sci Res **8**: 173–182

Gallois JL, Drouaud J, Lecureuil A, Guyon-Debast A, Bonhomme S, Guerche P (2013) Functional characterization of the plant ubiquitin regulatory X (UBX) domain-containing protein AtPUX7 in *Arabidopsis thaliana*. Gene **526**: 299–308

Ge W, Steber CM (2018) Positive and negative regulation of seed germination by the Arabidopsis GA hormone receptors, *GID1a, b, and c*. Plant Direct **2**: 1–11

Geissman TA, Verbiscar AJ, Phinney BO, Cragg G (1966) Studies on the biosynthesis of gibberellins from (−)-kaurenoic acid in cultures of *Gibberella fujikuroi*. Phytochemistry **5**: 933–947

Gietz RD, Woods RA (2002) Transformation of yeast by lithium acetate/single-stranded carrier DNA/polyethylene glycol method. Method Enzymol **350**: 87–896

Griffiths J, Murase K, Rieu I, Zentella R, Zhang ZL, Powers SJ, Gong F, Phillips AL, Hedden P, Sun TP, et al. (2006) Genetic characterization and functional analysis of the *GID1* gibberellin receptors in Arabidopsis. Plant Cell **18**: 3399–3414

Hauvermale AL, Ariizumi T, Steber CM (2012) Gibberellin signaling: a theme and variations on DELLA repression. Plant Physiol **160**: 83–92

Hauvermale AL, Ariizumi T, Steber CM (2014) The roles of the GA receptors GID1a, GID1b, and GID1c in sly1-independent GA signaling. Plant Signal Behav **9**: e28030

Hauvermale AL, Tuttle KM, Takebayashi Y, Seo M, Steber CM (2015) Loss of *Arabidopsis thaliana* seed dormancy is associated with increased accumulation of the GID1 GA hormone receptors. Plant Cell Physiol **56**: 1773–1785

Hauvermale AL, Steber CM (2020) GA signaling is essential for the embryo-to-seedling transition during Arabidopsis seed germination, a ghost story. Plant Signal Behav **15**: e1705028

Herrmann C, Horn G, Spaargaren M, Wittinghofer A (1996) Differential interaction of the Ras family GTP-binding proteins H-Ras, Rap1A, and R-Ras with the putative effector molecules Raf kinase and Ral-guanine nucleotide exchange factor. J Biol Chem **271**: 6794–6800

Hoppe T, Matuschewski K, Rape M, Schlenker S, Ulrich HD, Jentsch S (2000) Activation of a membrane-bound transcription factor by regulated ubiquitin/proteasome-dependent processing. Cell **102**: 577–586

Huang A, Tang Y, Shi X, Jia M, Zhu J, Yan X, Chen H, Gu Y (2020) Proximity labeling proteomics reveals critical regulators for inner nuclear membrane protein degradation in plants. Nat Commun **11**: 3284

Hussain A, Cao D, Cheng H, Wen Z, Peng J (2005) Identification of the conserved serine/threonine residues important for gibberellin-sensitivity of Arabidopsis RGL2 protein. Plant J **44**: 88–99

Itoh H, Matsuoka M, Steber CM (2003) A role for the ubiquitin 26S-proteosome pathway in gibberellin signaling. Trends Plant Sci **8**: 492–497

Iuchi S, Suzuki H, Kim YC, Iuchi A, Kuromori T, Ueguchi-Tanaka M, Asami T, Yamaguchi I, Matsuoka M, Kobayashi M, et al. (2007) Multiple loss-of-function of Arabidopsis gibberellin receptor AtGID1s completely shuts down a gibberellin signal. Plant J **50**: 958–966

Jacobsen SE, Olszewski NE (1993) Mutations at the *SPINDLY* locus of Arabidopsis alter gibberellin signal transduction. Plant Cell **5**: 887–896

Kang B-H, Busse JS, Dickey C, Rancour DM, Bednarek SY (2001) The Arabidopsis cell plate-associated dynamin-like protein, ADL1Ap, is required for multiple stages of plant growth and development. Plant Physiol **126**: 47–68

Karssen CM, Zagorski S, Kepczynski J, Groot SPC (1989) Key role for endogenous gibberellins in the control of seed germination. Ann Bot **63**: 71–80

Kim SI, Bong SP, Do YK, Song YY, Sang IS, Jong TS, Hak SS (2015) E3 SUMO ligase AtSIZ1 positively regulates SLY1-mediated GA signaling and plant development. Biochem J **469**: 299–314

Koornneef M, Hanhart CJ, van der Veen JH (1991) A genetic and physiological analysis of late flowering mutants in *Arabidopsis thaliana*. Mol Gen Genet **229**: 57–66

Koornneef M, Jorna ML, Brinkhorst-van der Swan DLCB, Karssen CM (1982) The isolation of abscisic acid (ABA) deficient mutants by selection of induced revertants in non-germinating gibberellin sensitive lines of *Arabidopsis thaliana* (L.) Heynh. Theor Appl Genet **61**: 385–393

Koornneef M, Vanderveen JH (1980) Induction and analysis of gibberellin sensitive mutants in *Arabidopsis thaliana* (L.) heynh. Theor Appl Genet **58**: 257–263

Kretzschmar FK, Mengel LA, Muller AO, Schmitt K, Blersch KF, Valerius O, Braus GH, Ischebeck T (2018) PUX10 is a lipid droplet-localized scaffold protein that interacts with CELL DIVISION CYCLE48 and is involved in the degradation of lipid droplet proteins. Plant Cell **30**: 2137–2160

Kurosawa E (1926) Experimental studies on the nature of the substance secreted by the "bakanae" fungus. Nat His Soc Form **16**: 213–227

Kushiro T, Okamoto M, Nakabayashi K, Yamagishi K, Kitamura S, Asami T, Hirai N, Koshiba T, Kamiya Y, Nambara E (2004) The Arabidopsis cytochrome P450 CYP707A encodes ABA 8′-hydroxylases: key enzymes in ABA catabolism. EMBO J **23**: 1647–1656

Laemmli UK (1970) Cleavage of structural proteins during the assembly of the head of bacteriophage T4. Nature **227**: 680–685

Lin PC, Pomeranz MC, Jikumaru Y, Kang SG, Hah C, Fujioka S, Kamiya Y, Jang JC (2011) The Arabidopsis tandem zinc finger protein AtTZF1 affects ABA- and GA-mediated growth, stress and gene expression responses. Plant J **65**: 253–268

Livak KJ, Schmittgen TD (2001) Analysis of relative gene expression data using real-time quantitative PCR and the $2-\Delta\Delta CT$ method. Methods **25**: 402–408

Livne S, Weiss D (2014) Cytosolic activity of the gibberellin receptor GIBBERELLIN INSENSITIVE DWARF1A. Plant Cell Physiol **55**: 1727–1733

Locascio A, Blázquez MA, Alabadí D (2013) Dynamic regulation of cortical microtubule organization through prefoldin-DELLA interaction. Curr Biol **23**: 804–809

Marshall RS, Hua ZH, Mali S, McLoughlin F, Vierstra RD (2019) ATG8-binding UIM proteins define a new class of autophagy adaptors and receptors. Cell **177**: 766–781

Marshall RS, Vierstra RD (2019) Dynamic regulation of the 26S proteasome: from synthesis to degradation. Front Mol Biosci **6**: 40

Mayers JR, Hu T, Wang C, Cárdenas JJ, Tan Y, Pan J, Bednarek SY (2017) SCD1 and SCD2 form a complex that functions with the exocyst and RabE1 in exocytosis and cytokinesis. Plant Cell **29**: 2610–2625

McGinnis KM, Thomas SG, Soule JD, Strader LC, Zale JM, Sun TP, Steber CM (2003) The Arabidopsis *SLEEPY1* gene encodes a putative F-box subunit of an SCF E3 ubiquitin ligase. Plant Cell **15**: 1120–1130

Mérai Z, Chumak N, García-Aguilar M, Hsieh T-F, Nishimura T, Schoft VK, Bindics J, Ślusarz L, Arnoux S, Opravil S, et al. (2014) The AAA-ATPase molecular chaperone Cdc48/p97 disassembles sumoylated centromeres, decondenses heterochromatin, and activates ribosomal RNA genes. Proc Natl Acad Sci USA **111**: 16166–16171

Meyer HH, Wang YZ, Warren G (2002) Direct binding of ubiquitin conjugates by the mammalian p97 adaptor complexes, p47 and Ufd1-Npl4. EMBO J **21**: 5645–5652

Murase K, Hirano Y, Sun TP, Hakoshima T (2008) Gibberellin-induced DELLA recognition by the gibberellin receptor GID1. Nature **456**: 459–463

Murashige T, Skoog FA (1962) A revised medium for rapid growth and bioassays with tobacco tiss culture. Physiol Plant **15**: 473–497

Nakajima M, Shimada A, Takashi Y, Kim YC, Park SH, Ueguchi-Tanaka M, Suzuki H, Katoh E, Iuchi S, Kobayashi M, et al. (2006) Identification and characterization of Arabidopsis gibberellin receptors. Plant J **46**: 880–889

Nelson SK, Steber CM (2016) Gibberellin hormone signal perception: down-regulating DELLA repressors of plant growth and development. *In* P Hedden, SG Thomas, eds, Annual Plant Reviews, The Gibberellins, Vol. **49**. John Wiley & Sons, Hoboken, NJ, pp 153–187

Nelson SK, Steber CM (2017) Transcriptional mechanisms associated with seed dormancy and dormancy loss in the gibberellin-insensitive *sly1-2* mutant of *Arabidopsis thaliana*. PLoS ONE **12**:1-32

Nemoto K, Ramadan A, Arimura G-I, Imai K, Tomii K, Shinozaki K, Sawasaki T (2017) Tyrosine phosphorylation of the GARU E3 ubiquitin ligase promotes gibberellin signaling by preventing GID1 degradation. Nat Commun **8**: 1004

Orme CM, Bogan JS (2012) The ubiquitin regulatory X (UBX) domain-containing protein TUG regulates the p97 ATPase and resides at the endoplasmic reticulum-golgi intermediate compartment. J Biol Chem **287**: 6679–6692

Park S, Rancour DM, Bednarek SY (2007) Protein domain-domain interactions and requirements for the negative regulation of Arabidopsis CDC48/p97 by the plant ubiquitin regulatory X (UBX) domain-containing protein, PUX1. J Biol Chem **282**: 5217–5224

Park S, Rancour DM, Bednarek SY (2008) In planta analysis of the cell cycle-dependent localization of AtCDC48A and its critical roles in cell division, expansion, and differentiation. Plant Physiol **148**: 246–258

Peng J, Carol P, Richards DE, King KE, Cowling RJ, Murphy GP, Harberd NP (1997) The Arabidopsis *GAI* gene defines a signaling pathway that negatively regulates gibberellin responses. Genes Dev **11**: 3194–3205

Rancour DM, Dickey CE, Park S, Bednarek SY (2002) Characterization of AtCDC48. Evidence for multiple membrane fusion mechanisms at the plane of cell division in plants. Plant Physiol **130**: 1241–1253

Rancour DM, Park S, Knight SD, Bednarek SY (2004) Plant UBX domain-containing protein 1, PUX1, regulates the oligomeric structure and activity of Arabidopsis CDC48. J Biol Chem **279**: 54264–54274

Rieu I, Ruiz-Rivero O, Fernandez-Garcia N, Griffiths J, Powers SJ, Gong F, Linhartova T, Eriksson S, Nilsson O, Thomas SG, et al. (2008) The gibberellin biosynthetic genes AtGA20ox1 and AtGA20ox2 act, partially redundantly, to promote growth and development throughout the Arabidopsis life cycle. Plant J Mol Biol **53**: 488–504

Rosnoblet C, Chatelain P, Klinguer A, Bègue H, Winckler P, Pichereaux C, Wendehenne D (2021) The chaperone-like protein Cdc48 regulates ubiquitin-proteasome system in plants. Plant Cell Environ **44**: 2636–2655

Salanenka Y, Verstraeten I, Löfke C, Tabata K, Naramoto S, Glanc M, Friml J (2018) Gibberellin DELLA signaling targets the retromer complex to redirect protein trafficking to the plasma membrane. Proc Natl Acad Sci USA **115**: 3716–3721

Sandhu KS, Koirala PS, Neff MM (2013) The *ben1-1* brassinosteroid-catabolism mutation is unstable due to epigenetic modifications of the intronic T-DNA insertion. G3 (Bethesda, MD) **3**: 1587–1595

Schneider CA, Rasband WS, Eliceiri KW (2012) NIH Image to ImageJ: 25 years of image analysis. Nat Methods **9**: 671–675

Schuberth C, Buchberger A (2008) UBX domain proteins: major regulators of the AAA ATPase Cdc48/p97. Cell Mol Life Sci **65**: 2360–2371

Seo PJ, Xiang F, Qiao M, Park JY, Lee YN, Kim SG, Lee YH, Park WJ, Park CM (2009) The MYB96 transcription factor mediates abscisic acid signaling during drought stress response in Arabidopsis. Plant Physiol **151**: 275–289

Serebriiskii I, Khazak V, Golemis EA (1999) A two-hybrid dual bait system to discriminate specificity of protein interactions. J Biol Chem **274**: 17080–17087

Silverstone AL, Mak PYA, Martínez EC, Sun TP (1997) The new *RGA* locus encodes a negative regulator of gibberellin response in *Arabidopsis thaliana*. Genetics **146**: 1087–1099

Shanmugabalaji V, Chahtane H, Accossato S, Rahire M, Gouzerh G, Lopez-Molina L, Kessler F (2018) Chloroplast biogenesis controlled by DELLA-TOC159 interaction in early plant development. Curr Biol **28**: 2616–2623

Shimada A, Ueguchi-Tanaka M, Nakatsu T, Nakajima M, Naoe Y, Ohmiya H, Kato H, Matsuoka M (2008) Structural basis for gibberellin recognition by its receptor GID1. Nature **456**: 520–523

Shimada A, Ueguchi-Tanaka M, Sakamoto T, Fujioka S, Takatsuto S, Yoshida S, Sazuka T, Ashikari M, Matsuoka M (2006) The rice *SPINDLY* gene functions as a negative regulator of gibberellin signaling by controlling the suppressive function of the DELLA protein, SLR1, and modulating brassinosteroid synthesis. Plant J Cell Mol Biol **48**: 390–402

Steber CM, Cooney SE, McCourt P (1998) Isolation of the GA-response mutant *sly1* as a suppressor of *ABI1-1* in *Arabidopsis thaliana*. Genetics **149**: 509–521

Swain SM, Tseng T-S, Olszewski NE (2001) Altered expression of *SPINDLY* affects gibberellin response and plant development. Plant Physiol **126**: 1174–1185

Takahashi N, Kitamura H, Kawarada A, Seta Y, Takai M, Tamura S, Sumiki Y (1955) Biochemical studies on "Bakanae" fungus: part XXXIV. Isolation of Gibberellins and their properties part XXXV. Relation between gibberellins, A1, A2, and gibberellic acid. J Agric Chem Soc Japan **19**: 267–281

Thomas SG, Blázquez MA, Alabadí D (2016) DELLA proteins: master regulators of gibberellin-responsive growth and development. *In* P Hedden, SG Thomas, eds, Annual Plant Reviews, The Gibberellins, Vol. **49**, John Wiley & Sons, Hoboken, NJ, pp 189–228

Ueguchi-Tanaka M, Ashikari M, Nakajima M, Itoh H, Katoh E, Kobayashi M, Chow TY, Hsing YIC, Kitano H, Yamaguchi I, et al (2005) *GIBBERELLIN INSENSITIVE DWARF1* encodes a soluble receptor for gibberellin. Nature **437**: 693–698

Ueguchi-Tanaka M, Hirano K, Hasegawa Y, Kitano H, Matsuoka M (2008) Release of the repressive activity of rice DELLA protein SLR1 by gibberellin does not require SLR1 degradation in the *gid2* mutant. Plant Cell **20**: 2437–2446

Ueguchi-Tanaka M, Matsuoka M (2010) The perception of gibberellins: clues from receptor structure. Curr Opin Plant Biol **13**: 503–508

Ueguchi-Tanaka M, Nakajima M, Katoh E, Ohmiya H, Asano K, Saji S, Hongyu X, Ashikari M, Kitano H, Yamaguchi I, et al. (2007) Molecular interactions of a soluble gibberellin receptor, GID1, with a rice DELLA protein, SLR1, and gibberellin. Plant Cell **19**: 2140–2155

Van Leene J, Eeckhout D, Persiau G, Van De Slijke E, Geerinck J, Van Isterdael G, Witters E, De Jaeger G (2011) Isolation of transcription factor complexes from Arabidopsis cell suspension cultures by tandem affinity purification. *In* Lyuan, S Perry, eds, Plant Transcription Factors. Methods in Molecular Biology (Methods and Protocols), Vol. **754**. Humana Press, Totowa, NJ, pp 195–218

Walhout AJM, Vidal M (2001) High-throughput yeast two-hybrid assays for large-scale protein interaction mapping. Methods **24**: 297–306

Wang F, Zhu D, Huang X, Li S, Gong Y, Yao Q, Fu X, Fan LM, Deng XW (2009) Biochemical insights on degradation of Arabidopsis DELLA proteins gained from a cell-free assay system. Plant Cell **21**: 2378–2390

Willige BC, Ghosh S, Nill C, Zourelidou M, Dohmann EM, Maier A, Schwechheimer C (2007) The DELLA domain of GA INSENSITIVE mediates the interaction with the GA INSENSITIVE DWARF1A gibberellin receptor of Arabidopsis. Plant Cell **19**: 1209–1220

Woodman PG (2003) p97, a protein coping with multiple identities. J Cell Sci **116**: 4283–4290

Xu P, Chen H, Li T, Xu F, Mao Z, Cao X, Miao L, Du S, Hua J, Zhao J, et al. (2021) Blue light-dependent interactions of CRY1 with GID1 and DELLA proteins regulate gibberellin signaling and photomorphogenesis in Arabidopsis. Plant Cell **33**: 2375–2394

Yamamoto Y, Hirai T, Yamamoto E, Kawamura M, Sato T, Kitano H, Matsuoka M, Ueguchi-Tanaka M (2010) A rice *gid1* suppressor mutant reveals that gibberellin is not always required for interaction between its receptor, GID1, and DELLA proteins. Plant Cell **22**: 3589–3602

Yamauchi Y, Ogawa M, Kuwahara A, Hanada A, Kamiya Y, Yamaguchi S (2004) Activation of gibberellin biosynthesis and response pathways by low temperature during imbibition of *Arabidopsis thaliana* seeds. Plant Cell **16**: 367–378

Yan B, Yang Z, He G, Jing Y, Dong H, Ju L, Zhang Y, Zhu Y, Zhou Y, Sun J (2021) The blue light receptor CRY1 interacts with GID1 and DELLA proteins to repress gibberellin signaling and plant growth. Plant Commun **2**: 100245

Yoshida H, Hirano K, Sato T, Mitsuda N, Nomoto M, Maeo K, Koketsu E, Mitani R, Kawamura M, Ishiguro S, et al. (2014) DELLA protein functions as a transcriptional activator through the DNA binding of the Indeterminate Domain family proteins. Proc Natl Acad Sci USA **111**:7861–7866

Zentella R, Zhang ZL, Park M, Thomas SG, Endo A, Murase K, Fleet CM, Jikumaru Y, Nambara E, Kamiya Y, Sun TP (2007) Global analysis of DELLA direct targets in early gibberellin signaling in Arabidopsis. Plant Cell **19**: 3037–3057

Zhang J, Vancea AI, Hameed UFS, Arold ST (2021) Versatile control of the CDC48 segregase by the plant UBX-containing (PUX) proteins. Comput Struct Biotechnol J **19**: 3125–3132

Zhong M, Zeng BJ, Tang DY, Yang JX, Qu LN, Yan JD, Wang XCA, Li X, Liu XM, Zhao XY (2021) The blue light receptor CRY1 interacts with GID1 and DELLA proteins to repress GA signaling during photomorphogenesis in *Arabidopsis*. Mol Plant **14**: 1328–1342

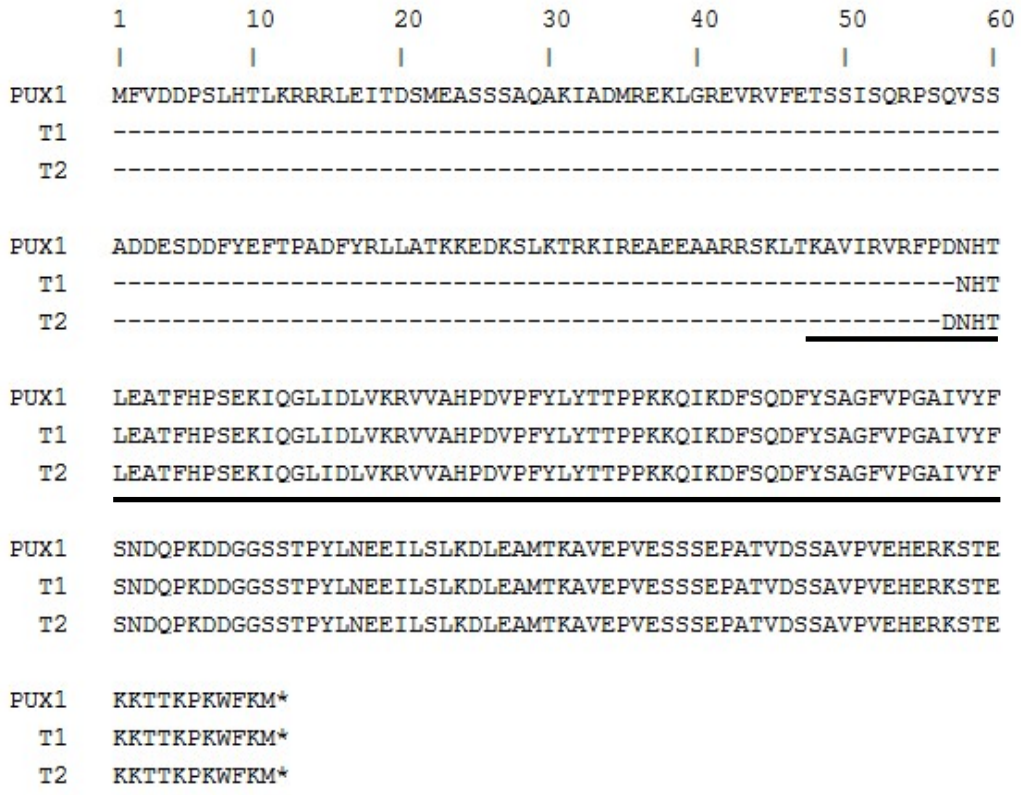

Supplemental Figure S1. Amino acid sequence alignment of PUX1 and truncated transformants T1 and T2 isolated from the yeast two-hybrid screen. Dashed lines represent the missing amino acid sequences from the two recovered PUX1 transformants. The solid bar indicates the amino acid sequence of the ubiquitin binding (UBX) domain present in full-length PUX1 and truncated yeast two-hybrid PUX1 isolates.

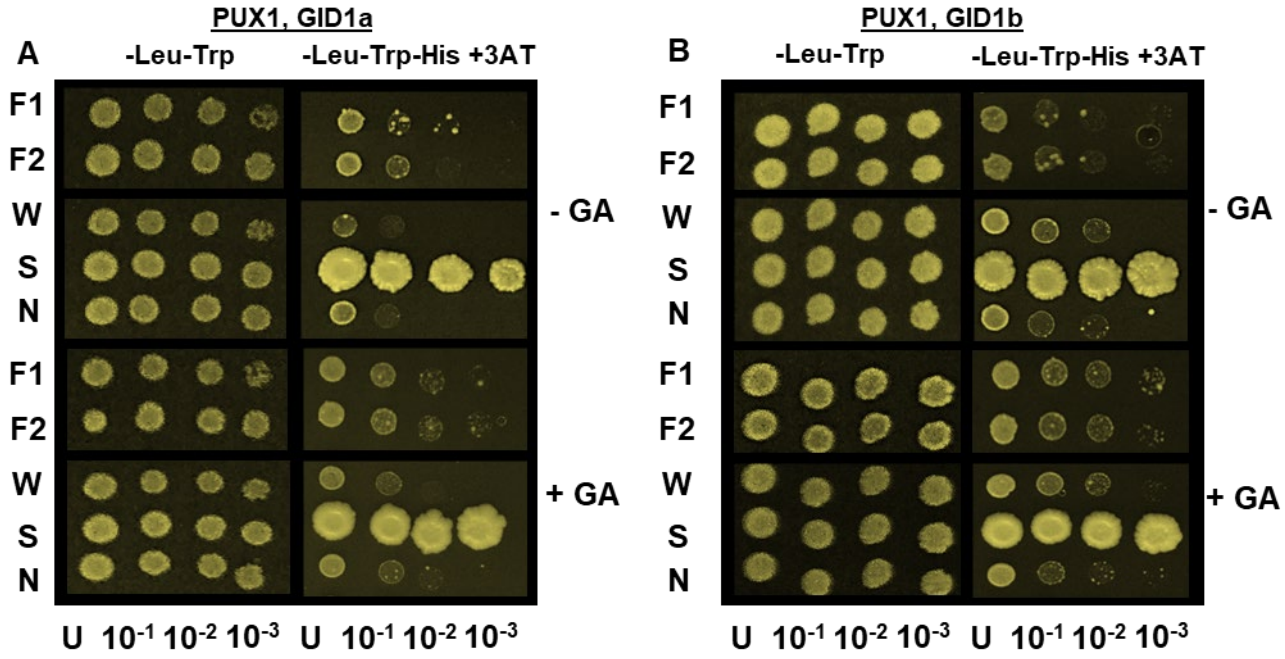

Supplemental Figure S2. Detection of *in vivo* interactions between GID1 and PUX1 proteins in bait prey swaps. In yeast two-hybrid experiments, full-length PUX1 bait constructs interacted with full-length (A) GID1a and (B) GID1b proteins fused to the Gal4 DNA binding domain interact with or without 10 μM GA_3. F1 and F2 represent two independent transformants expressing full-length *PUX1* constructs. Yeast samples were plated as undiluted (U) samples and at dilutions of 1/10 (10^{-1}), 1/100 (10^{-2}), and 1/1000 (10^{-3}) on synthetic dextrose media without leucine and tryptophan (-Leu-Trp), or without leucine, tryptophan, and histidine, and with 10 mM 3AT (-Leu-Trp-His + 3AT), and in the presence or absence of GA. Controls included with each screen are a weak interaction control (W), a strong interaction control (S), and a negative interaction control (N).

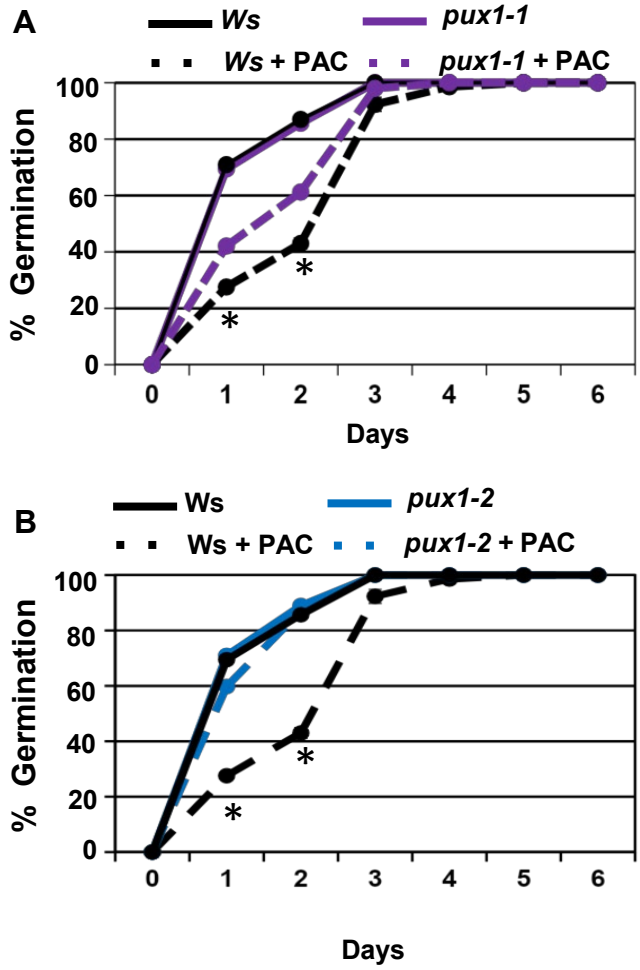

Supplemental Figure S3. Mutant *pux1* seeds display decreased sensitivity to GA inhibitor paclobutrazol (PAC). Ws, (A) *pux1-1,* and (B) *pux1-2* seeds were imbibed at 4ºC with or without 0.5 µM PAC for 24 hours, washed 3 times with water, plated on 0.5 X MS agar and germinated in the light at 22ºC. Germination was scored daily. Percent germination is the average of three biological replicates, and n=100. Statistical significance was determined by analysis of variance (ANOVA) using a Tukey's pairwise comparison, and p-values of <0.05 are indicated with an asterisk (*).

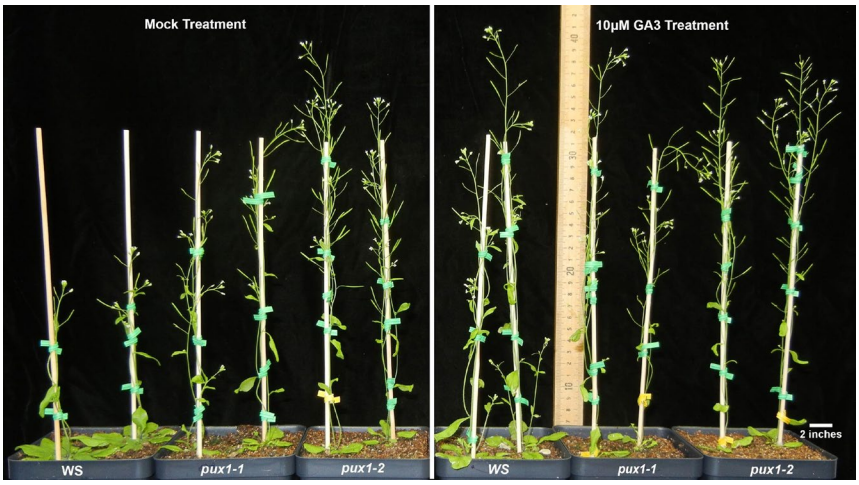

Supplemental Figure S4. Loss-of-function *pux1* mutants are non-responsive to exogenous GA. Aerial portions of mock or 10 μM GA_3 treated 33-d-old wild-type *pux1-1* and *pux1-2* mutant plants . All plants were homozygous for the genotype(s) indicated. Plants were sprayed with either 10 μM GA_3 or mock treatment once per week. Mutant *pux1* plants bolted faster than wild type, but their final heights were similar to wild-type plants **(Fig 3B, C).**

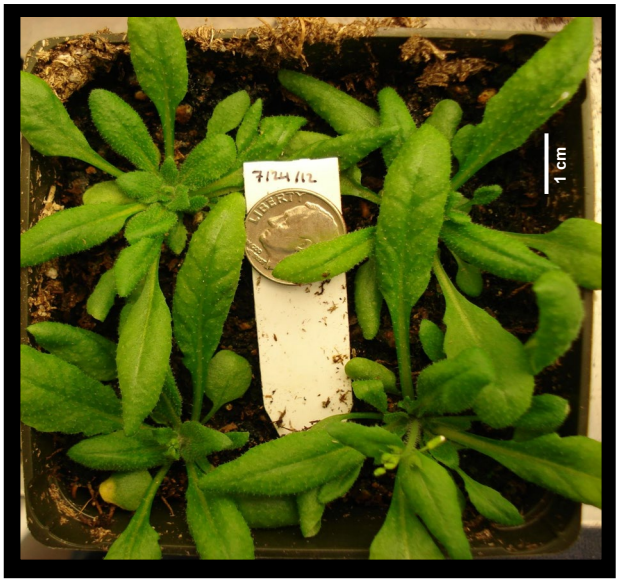

Supplemental Figure S5. At 32 days after germination (DAG), Ws WT has just transitioned to flowering

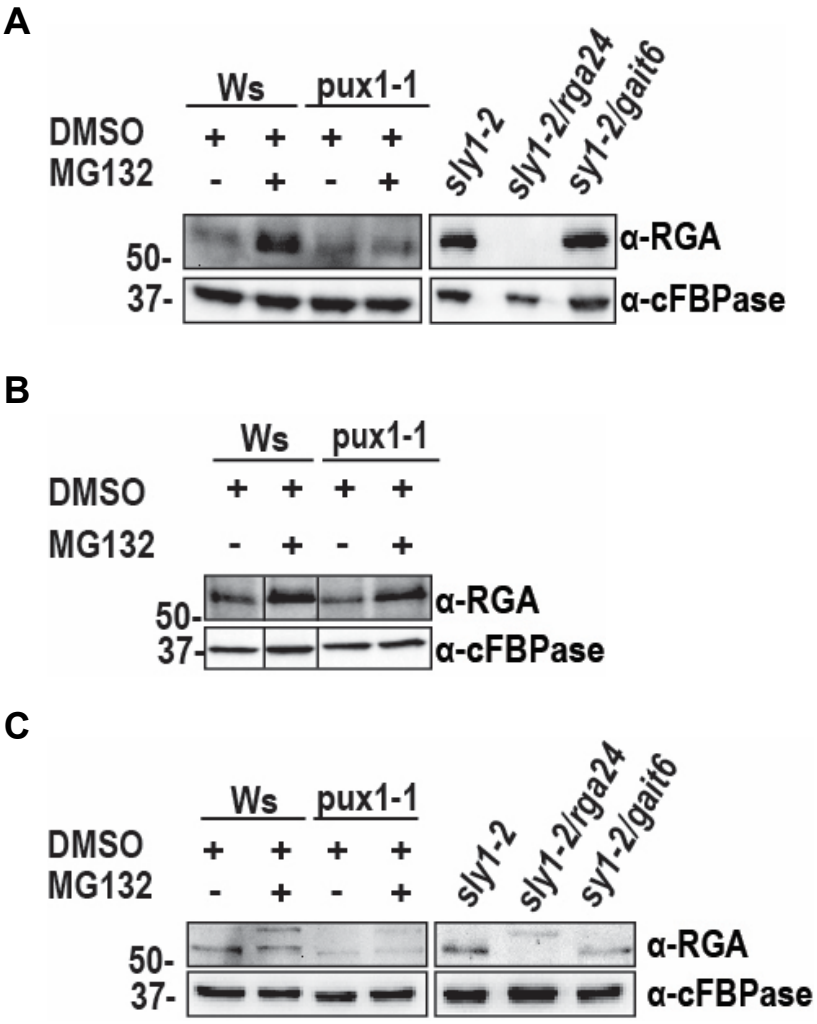

Supplemental Figure S6. Immunoblot analysis of DELLA protein levels in *pux1-1* and wild type seedlings. (A, B, C) Immunoblots of total protein extracts from Ws WT and *pux1-1* mutant 5-d-old seedlings treated with MG132 or DMSO used for quantitation of RGA protein levels in Fig. 6B. Total protein extracts of *sly1-2* and *sly1-2*/*rga-24* and *sly1-2*/*gai-t6* double mutant seedlings were analyzed in parallel to confirm the identity of the polypeptide detected by immunoblotting with anti-RGA antibodies in Ws WT and *pux1-1* protein extracts. cFBPase was detected as a loading control. 20 µg total protein was loaded per lane.

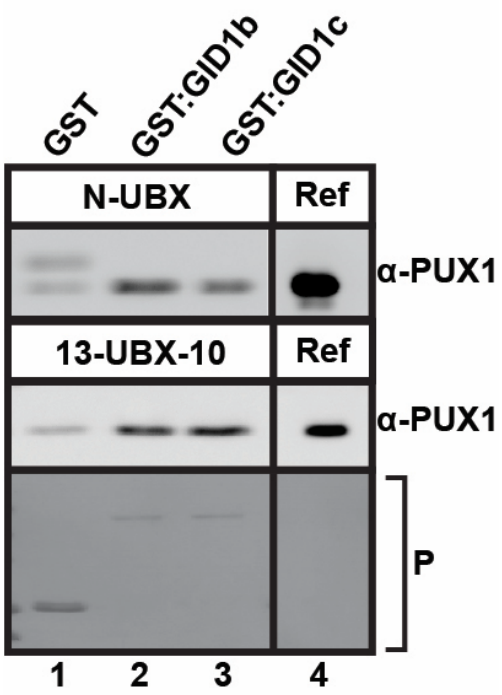

Supplemental Figure S7. Binding of the PUX1 UBX domain to GID1 is not affected by the presence of GA. *In vitro a*nalysis of GST-GID1b and GST-GID1c binding to truncated PUX1 proteins containing the UBX domain in the presence of GA . Purified GST (lane 1) or GST-GID1b,c (lane 2,3) were incubated with tag-free N-UBX, or 13.UBX.10, of PUX1 in the presence of GA. Input lane of purified respective PUX1 truncation proteins (lane 4) was used as a control. Ponceau Stain (P) was used to visualize input protein.

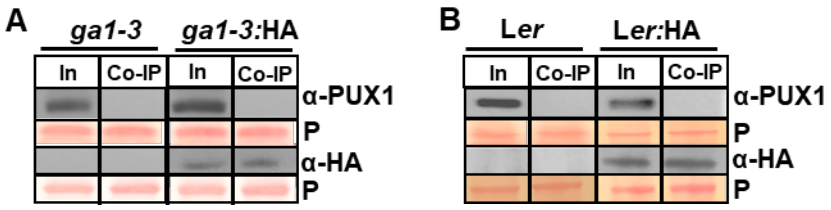

Supplemental Figure S8: Validation of anti-HA antibody specificity: Anti-HA antibodies did not immunoprecipitate PUX1 protein. (A, B) Immunoblot analysis of total (Input; IN) and anti-HA immunoprecipitated (co-IP) proteins from untransformed *ga1-3* seeds and transgenic *ga1-3* HA seeds expressing the HA epitope. Seeds were imbibed at 4ºC for 3 days and then moved to 22ºC in the light for 2 days. 60 µg of seed protein extracts were incubated with α-HA magnetic beads and PUX1 protein was detected with anti-PUX1 primary antibody (1:5000), and anti-rabbit HRP secondary antibody (Sigma; 1:10,000). Protein loading was visualized with Ponceau (P). HA was detected with anti-HA primary antibody (1:5000), and anti-rabbit HRP secondary antibody (Sigma; 1:10,000).

A = Arabidopsis Protoplast
B = T87 Arabidopsis-cultured cells

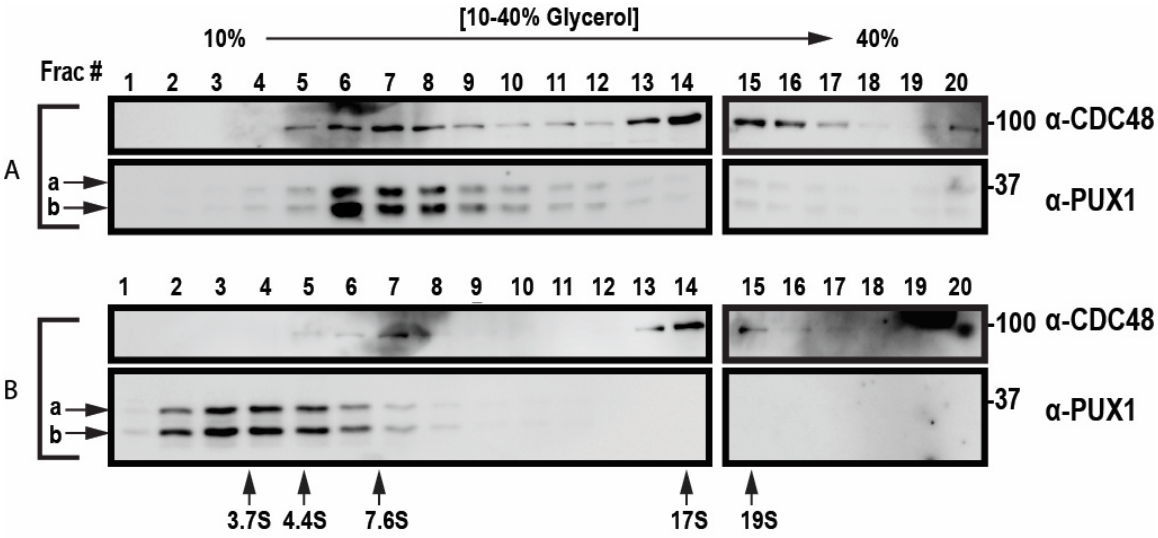

Supplemental Figure S9. Differences in the velocity sedimentation profile of PUX1 and CDC48a in cell extracts from T87 protoplasts and T87 suspension-cultured cells. Immunoblot analysis of total protein extracts from T87 protoplasts (A) and T87 suspension-cultured cells (not protoplasted) (B) were fractionated by velocity sedimentation centrifugation. For preparation of protein extracts, protoplasts were lysed by extrusion through a 25-gauge needle whereas T87 suspension-cultured cells were lysed using a N_2 cell disrupter. 500 µg of total protein extract was fractionated by centrifugation on a 10% to 40% glycerol gradient. Arrows indicate fractionation of molecular mass standards with their indicated Svedberg (S)-values.

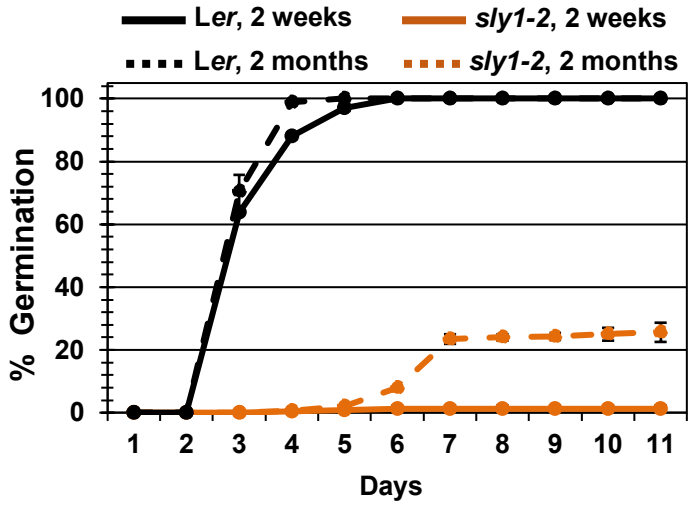

Supplemental Figure S10. Germination efficiency of dormant and after-ripened L*er* WT and *sly1-2* seeds used to generate the yeast two-hybrid cDNA library. The yeast two-hybrid cDNA library used for screen for GID1 interactors was made from wild-type L*er* and *sly1-2* mutant seeds which display differences in dormancy with genotype and with after-ripening. Seeds were harvested at physiological maturity when siliques turned yellow, and then after-ripened for 2 weeks (solid line) or for 2 months (dotted line) at room temperature before storage at -20°C to slow further after-ripening. Seeds were plated on MS-agar and imbibed at 4°C for 3 d, and then moved to 22°C in the light for 11 d. Germination was scored daily until seeds stopped germinating. Percent germination is the average of three biological replicates, and n=100. Error bars = SD.

Supplemental Table S1. Yeast Two-Hybrid screen summary.

Two-Hybrid Screen	Total
Transformants	8.97×10^7
Putative Clones	2820
Clones Retested	221
Interaction Score (3-5)	90
GA-Enhanced	22

GA = 10 μM GA_3

Supplemental Table S2. List of GID1b interactors.

Gene	Name
AT1G03880	CRU2
AT1G04410	C-NAD-MDH1
AT1G04560	AWPM-19-like
AT1G05340	Unknown function
AT1G07920	GTP binding Elongation Factor Tu
AT1G07950	MED22B
AT1G07985	Unknown function
AT1G08360	L1p/L10e
AT1G12440	A20/AN1-like zinc finger family
AT1G13280	AOC4
AT1G14980	CPN10
AT1G15100	RING-H2 finger protein RHA2a
AT1G17100	SOUL heme-binding family
AT1G19540	NmrA-like
AT1G21460	ATSWEET1
AT1G26470	Unknown function
AT1G27990	Unknown function
AT1G44446	CHLORINA1
AT1G52730	TransducinWD40 repeat like
AT1G52930	Ribosomal RNA Brix domain protein
AT1G53750	RT1A
AT1G54100	ALDH7B4
AT1G54860	GPI-anchored Glycoprotein
AT1G60420	Reduce transmission through pollen
AT1G66510	AAR2 protein family
AT1G67120	ATPases
AT1G68250	Unknown function
AT1G70840	MLP-like protein 31 (MLP31)
AT1G73190	ALPHA-TIP
AT1G74670	GASA6
AT1G75630	AVA-P4
AT1G75830	LCR67 (PR) protein
AT1G77680	Ribonuclease 11/R family protein
AT1G77770	Zinc binding function unknown
AT1G77920	bZIP transcription factor family
AT1G78040	Pollen Ole e1
AT1G78380	ATGSTU19 (TAU 19)
AT2G02120	LCR70
AT2G05580	Glycine-rich protein family
AT2G15690	TPR-like superfamily protein
AT2G15890	MEE14
AT2G17250	EMB2762
AT2G18510	EMB2444
AT2G20490	NOP10 (EDA27)

Gene	Name
AT2G21490	LEA dehydrin
AT2G21820	Unknown function
AT2G23090	Unknown function (SERF)
AT2G26355	Potential natural antisense gene Ribosomal
AT2G27530	protein L10aP (PGY1)
AT2G27940	RING/U-box superfamily
AT2G34360	MATE efflux family protein
AT2G35300	LEA4-2/LEA18
AT2G40170	LEA, ATEM6
AT2G41260	ATM17
AT2G44860	Ribosomal protein L24e
AT2G44990	ATCCD7 (MAX3)
AT2G45510	CYP704A
AT2G47770	AtTSPO
AT3G01570	Oleosin family protein
AT3G02200	PCI domain protein
AT3G06420	ATG8H
AT3G07780	OBE1
AT3G08505	Zinc finger C3HC4-type RING
AT3G09440	HSP 70
AT3G09890	Ankyrin repeat family
AT3G11500	Small nuclear ribonuclear protein
AT3G14660	CYP72A13
AT3G15660	Glutathoredoxin 4 (GTX 4)
AT3G20480	ATLPXK
AT3G22640	PAP85
AT3G22900	NRPD7
AT3G27310	PUX1
AT3G27660	OLEO4
AT3G48510	Unknown function
AT3G49910	SH3-like
AT3G50970	LT130, XERO2
AT3G50980	XERO1
AT3G56150	EIF3c
AT3G57290	EIF3e (INT-6)
AT4G09800	RPS18C
AT4G13850	ATGRP2
AT4G14720	PPD2, TIFY4B
AT4G18650	Unknown function (maternal)
AT4G22820	A20/AN1-like zinc finger family
AT4G25140	OLEO1
AT4G27140	SESA1
AT4G27150	SESA2
AT4G27160	SEAS3

Gene	Name
AT4G28520	CRU3
AT4G28528	Unknown function
AT4G30650	Low temp and salt response
AT4G30910	Cytosol aminopeptidase family
AT4G30990	ARM repeat superfamily
AT4G31700	RPS6
AT4G33467	Unknown function
AT4G34881	Unknown function
AT4G38740	ROC1
AT4G39130	Dehydrin family protein
AT5G02960	S12/S23
AT5G03940	54 Chloroplast protein
AT5G06190	Unknown function
AT5G06760	LEA4-5
AT5G07090	Ribosomal protein (S4)
AT5G10940	Transducin family (WD-40)
AT5G12030	ATHSP17.6A
AT5G21280	Hydroxyproline-rich glycoprotein
AT5G21940	Unknown function
AT5G22440	L1p/L10e family
AT5G22750	DNA repair (RAD5)
AT5G26742	EMB1138
AT5G27850	L18e/L15
AT5G35660	Glycine-rich protein
AT5G40340	Tudor/PWWP/MBT
AT5G40370	GRXC2
AT5G40420	OLEO1
AT5G44120	CRU1
AT5G47030	Mitochondrial ATP synthase δ
AT5G50700	HSD1
AT5G54740	SESA5
AT5G57550	XTR3
AT5G58070	ATTIL LIPOCALIN
AT5G58420	RPS4A
AT5G59170	Proline-rich extension-like family
AT5G59400	Unknown function
AT5G61220	LYR family Fe/S cluster
AT5G61820	Unknown function
AT5G65207	Unknown function
AT5G66400	Dehydrin RAB18
AT5G66760	SDH1-1
AT5G66780	Unknown function
AT5G67220	FMN-linked oxidoreductase
AT5G67600	WIH1 unknown function

Supplemental Table S3. Antibodies used in this study.

Antibodies	Clonality	Primary Dilution Immunoblot	Secondary HRP	Secondary Dilution	Citation
anti-GID1c	Polyclonal	1:1000	Rabbit	1:5000	Agrisera (AS14), Hauvermale et al., 2015
anti-PUX1	Polyclonal	1:5000	Rabbit	1:5000	Rancour et al., 2004
anti-CDC48a	Polyclonal	1:500	Chicken	1:5000	Rancour et al., 2004
anti-cFBPase	Polyclonal	1:5000	Rabbit	1:5000	Agrisera (AS04043)
anti-PAP	Polyclonal	1:2500		N/A	SigmaAldrich (P1291)
anti-HA	Polyclonal	1:5000	Rabbit (HRP)	1:10,000	Immuno Consultants Laboratory (RHGT-45A-Z) Hauvermale et al., 2015
anti-RGA	Polyclonal	1:1000	Rabbit	1:5000	Agrisera (AS11) Leone et al., 2014

Supplemental Table S4. Primers used in this study.

Primer Names	Primer Sequence	Purpose	Citation
GID1a SYB Forward Primer	GAAATGGCTGCGAGCGATGAAG	RT-qPCR	
GID1a SYB Reverse Primer	ATTGAGAGGAACCACTGTTCTGC	RT-qPCR	
GID1b SYB Forward Primer	TGGAGACTATGGCTGGTGGTAAC	RT-qPCR	
GID1b SYB Reverse Prime	AGTGGGACAATTCTCTTGCATTCG	RT-qPCR	
GID1c SYB Forward Primer	TCTTCGATCTGGGCTTTCGTGTC	RT-qPCR	
GID1c SYB Reverse Primer	ATTGAGAGGAACCACTGTCTTGC	RT-qPCR	
GID1a Forward Seq. Primer	TCCCAGTCACGACGTTGTAAAAC	Sequencing	
GID1a Reverse Seq. Primer	AACAGCTATGACCATG	Sequencing	
GID1b/c Forward Seq. Primer	TCCCAGTCACGACGTTGTAAAAC	Sequencing	
GID1b/c Reverse Seq. Primer	TAAGGCTAGAGTACTTAATACGACT CACTATAGG	Sequencing	
AHBaitForward	AACCGAAGTGCGCCAAGTGTCTG	Bait plasmid sequencing	
AHPreyForward	TATAACGCGTTTGGAATCACT	Prey plasmid sequencing	
AHBaitPreyReverse	AGCCGACAACCTTGATTGGAGAC	Bait/Prey plasmid sequencing	
AtGID1a-OrfF	ATGGCTGCGAGCGATGAAGT	Cloning/Sequencing	Ariizumi et al., 2008
AtGID1a-OrfR	TTAACATTCCGCGTTTACAAACGCC GAA	Cloning/Sequencing	Ariizumi et al., 2008
AtGID1b-OrfF	ATGGCTGGTGGTAACGAAGT	Cloning/Sequencing	Ariizumi et al., 2008
AtGID1b-OrfR	CTAAGGAGTAAGAAGCACAG	Cloning/Sequencing	Ariizumi et al., 2008
PUX1F	ATGTTTGTTGATGACCCTTCTC	5'-PUX1 Cloning/Sequencing	Rancour et al., 2004
PUX1R	TCACATTTTAAACCACTTAGGC	3'-PUX1 Cloning/Sequencing	Rancour et al., 2004
RGA Forward	TGGCCAAGGTTATCGTGTGGAG	RT-qPCR	
RGA Reverse	ACGAGTGTGCCAACCCAACATC	RT-qPCR	
GAI Forward	TCACCGACCTTAATCCTCCGT	RT-qPCR	
GAI Reverse	CGAATCGATAGCGAACTGATTG	RT-qPCR	
UBC18 Forward	ACCCAGTCGGTGGATTTACTTGC	RT-qPCR	
UBC18 Reverse	GAAATGGCTGCGAGCGATGAAG	RT-qPCR	
TUB5 Forward	CTCAGCACTCCTAGCTTTGGAGAC	RT-qPCR	
TUB5 Reverse	TTAGGTTCACCGCGAGTTTCCTG	RT-qPCR	